INFORMATION TO USERS

This dissertation was produced from a microfilm copy of the original document. While the most advanced technological means to photograph and reproduce this document have been used, the quality is heavily dependent upon the quality of the original submitted.

The following explanation of techniques is provided to help you understand markings or patterns which may appear on this reproduction.

1. The sign or "target" for pages apparently lacking from the document photographed is "Missing Page(s)". If it was possible to obtain the missing page(s) or section, they are spliced into the film along with adjacent pages. This may have necessitated cutting thru an image and duplicating adjacent pages to insure you complete continuity.

2. When an image on the film is obliterated with a large round black mark, it is an indication that the photographer suspected that the copy may have moved during exposure and thus cause a blurred image. You will find a good image of the page in the adjacent frame.

3. When a map, drawing or chart, etc., was part of the material being photographed the photographer followed a definite method in "sectioning" the material. It is customary to begin photoing at the upper left hand corner of a large sheet and to continue photoing from left to right in equal sections with a small overlap. If necessary, sectioning is continued again — beginning below the first row and continuing on until complete.

4. The majority of users indicate that the textual content is of greatest value, however, a somewhat higher quality reproduction could be made from "photographs" if essential to the understanding of the dissertation. Silver prints of "photographs" may be ordered at additional charge by writing the Order Department, giving the catalog number, title, author and specific pages you wish reproduced.

University Microfilms

300 North Zeeb Road
Ann Arbor, Michigan 48106

A Xerox Education Company

THE UNIVERSITY OF OKLAHOMA

GRADUATE COLLEGE

GEOCHEMISTRY AND PETROLOGY OF SOME OKLAHOMA REDBED COPPER OCCURRENCES

A DISSERTATION

SUBMITTED TO THE GRADUATE FACULTY

in partial fulfillment of the requirements for the

degree of

DOCTOR OF PHILOSOPHY

BY

RICHARD PATRICK LOCKWOOD

Norman, Oklahoma

1972

GEOCHEMISTRY AND PETROLOGY OF SOME OKLAHOMA

REDBED COPPER OCCURRENCES

APPROVED BY

Charles J. Mankin

Muriel L. Thom

Howard W. Day

Kenneth S. Johnson

DISSERTATION COMMITTEE

GEOCHEMISTRY AND PETROLOGY OF SOME OKLAHOMA REDBED COPPER OCCURRENCES

ABSTRACT

Two copper-rich shales are now undergoing development or mining in southwestern Oklahoma, the Mangum deposit in Ts. 3 and 4 N., R. 22 W., and the Creta deposit in Ts. 1 and 2 S., R. 22 W. Both deposits are in the upper part of the Permian Flowerpot Formation, which consists mainly of reddish shales with interbeds of gray shale, gypsum, and dolomite. The Flowerpot Formation is in the El Reno Group and Leonardian in age.

A total of 226 samples of ore and non-ore rock were collected or donated: 108 samples are from Mangum and 118 (including 65 pulped cores) are from Creta. Samples were analyzed for quartz, gypsum, K_2O, CaO, Ag, Pb, V, Co, Ni, total iron as Fe_2O_3, CuO, ZnO, U, and MoO_3 by x-ray methods, for illite, chlorite, and malachite (Mangum) or chalcocite (Creta) by calculation, and for organic matter by standard wet chemical methods. Two samples of bedded gypsum imme-

diately overlying the Creta ore and seven chalcocite concentrates were run for $\delta\,^{34}S/^{32}S$.

The patterns of correlation coefficients are very similar for shales of the same color in each deposit and for each deposit as a whole. Exceptions are correlations of U with illite, chlorite, Ag, V, Co, Fe_2O_3, K_2O, and CaO in the Mangum deposit. There are 2 sets of correlations in each deposit: positive correlations between K_2O and Co, Ni, V, Ag, Fe_2O_3 (and ZnO, Mangum) and negative correlations between gypsum and the same metals. The negative set are interpreted to be products of illite dilution by gypsum. The positive set are interpreted as being due to the structural or interlayer position of these metals in illite in both deposits.

Sulfur isotope analyses revealed a wide range of $\delta\,^{34}S/^{32}S$ values for chalcocite samples, and higher, more uniform values for gypsum samples. This is consistent with the possible bacteriogenic origin of the sulfide. Since there are no horizontal lead and zinc zones of the Schurmann variety, the chalcocite at Creta is interpreted to be diagenetic. The copper mineral in the Mangum deposit is predominantly malachite; the overburden is thinner than at Creta, and the Mangum deposit is interpreted as being the oxidized analog of the Creta deposit.

ACKNOWLEDGMENTS

During a research project of the type and duration of this one, it is inevitable that the researcher would have much aid to acknowledge. This project, indeed even the occurrence of copper-rich shales in Oklahoma, was brought to my attention by Dr. C. J. Mankin. For this, as well as directing the project, I am especially indebted to Dr. Mankin. I would like to acknowledge my debt to the members of my committee, Drs. George T. Stone, Howard W. Day, and Kenneth S. Johnson, for their help and patience.

Without the permission of the management of Eagle-Picher Industries, Inc., and Lobaris Copper Co., Inc., to visit and sample the Creta and Mangum deposits, respectively, the project would never have been started. My thanks are due to Douglas C. Brockie, P. R. Dingess, and Paul Jones of Eagle-Picher Industries, Inc., and to Robert W. Allen and John H. Warren of Lobaris Copper Co., Inc.

Special thanks are due to Dr. M. L. Jensen of the University of Utah, for his interest and for doing the

sulfur isotope analyses. I am also happy to acknowledge my debt to Mr. Harry F. Robertson of the Bartlesville, Oklahoma, office of the U. S. Bureau of Mines and to the Geological Society of America, Inc. (Penrose Bequest Research Grant 1299-69) for financial aid.

Dr. C. W. Harper, Jr., helped me do some statistical calculations. William H. Bellis tried valiantly to keep the x-ray fluorescence unit I needed operating; I am sure that he is glad that the writing stage has arrived. The aid of both gentlemen is appreciated.

David M. Patrick, Garrett L. Morrison, and Ben D. Hare have all helped in many ways--I am particularly grateful for their generosity when we were sharing the same instruments.

Finally, the work would never have been completed without the continual encouragement of my wife, Mary.

CONTENTS

TABLES

ILLUSTRATIONS

GEOCHEMISTRY AND PETROLOGY OF SOME OKLAHOMA REDBED COPPER OCCURRENCES

INTRODUCTION

Purpose of Investigation

The purpose of this research is to relate the geochemistry and mineralogy of Oklahoma redbed copper occurrences and interpretations of Oklahoma geology to (1) the class characteristics of heavy metal deposits in redbeds, (2) deposition of heavy metals and their minerals from natural-water solutions, (3) sulfur isotope data, and (4) the trace-element composition of shales. The general approach has consisted of gathering data on the mineralogy and geochemistry of copper-shale occurrences in Oklahoma, and relating the data to the stratigraphy (Ham and Johnson, 1964; Ward, 1963) and other features, including paleoclimatic indicators (Wilson, 1962; Clapham, 1970), of the Permian Flowerpot shale.

There are a number of reasons why this study is appropriate now. Data on the trace element composition of

muddy sediments are now available, and the data are subdivided according to outstanding properties or environment of deposition (Krauskopf, 1955; Love, 1961; Davidson and Lakin, 1961; Vine, 1966, 1969; Vine and others, 1969). Also investigations have recently been made of the value of trace elements in muddy sediments as indicators of marine or nonmarine deposition (Shimp and others, 1969).

Secondly, it is now apparent that previous methods of attacking this problem, the origin of redbed metal occurrences, have not succeeded. Experimental syntheses of minerals have shown that the minerals present in this class of occurrences could have formed at low temperatures and pressures (Schmitt, 1962; Gaucher, 1964; Cuthbert, 1962; Roberts, 1963; Temple and LeRoux, 1964), but this has not enabled us to interpret the environment of formation. Detailed examination of metallic mineral textures has revealed little in the past except that the grains of metallic minerals have many habits (Trask, 1925) or are pseudomorphs (Love, 1962). This microscopic examination has further revealed that the metallic minerals involved either mimic or produce small structural features such as cross-bedding and microfaults in minute detail (White and Wright, 1954; Solomon, 1962).

Nature of Redbed Copper Deposits

Two hypotheses have been used to explain the origin of the redbed heavy-metal occurrences. These may be distinguished as the "syngenetic hypotheses" and the "epigenetic hypothesis" (Fischer, 1937).

The thesis of the syngenetic hypothesis is that the metals were deposited at the same time as the detrital grains making up the host rock. Variations of this hypothesis are that the deposition of metals results from inorganic precipitation, organically induced precipitation, deposition of clastic metallic minerals, or adsorption of metal ions and complexes on mineral grains or organic matter (Richardson and Hawkes, 1958; Slowey and Jeffrey, 1967). The source of metals is ascribed variously to volcanic exhalations or hydrothermal emanations into depositional basins, and to normal concentration of metals in sea water.

According to the epigenetic hypothesis, metals were deposited in the host rock from fluids that moved through the rock after it had been deposited. The 2 main variations of this hypothesis differ on the origin of the fluid: (1) hydrothermal waters, or (2) ground water (White, 1960; Noble, 1963). Another variant includes epigenetic concen-

tration of metals dispersed in sediments through normal syngenetic processes (Fischer, 1937).

An intermediate between the syngenetic and epigenetic hypotheses is diagenesis. Metal deposition in unconsolidated sediment would follow diffusion transport of the metal across the sediment-water interface (Kalliokoski, 1966).

Heavy metal deposits in sedimentary rocks include examples of metal-rock associations that are repeated many times worldwide. Uranium, for instance, is characteristically associated with ancient conglomerates (Davidson, 1964), black shales (Krauskopf, 1955), phosphorites (Park and MacDiarmid, 1964), and terrestrial sandstones (Fischer, 1937). Some associations are sufficiently common as to suggest that they are genetic: for example, the redbed copper shales and sandstones, the uranium-vanadium-rich terrestrial sandstones, and the metal-bearing bituminous shales (Davidson, 1964).

Redbed copper deposits have many class characteristics, some of which are peculiar: they occur principally in rocks of 3 geologic ages; they are widely distributed; and although they are named for the association of copper with red-colored sedimentary rocks, the metals are present primarily in non-red rocks.

There were apparently only 3 principal periods in earth history during which conditions were favorable for the formation of sediments rich in non-detrital copper. Known occurrences all belong to 1 of the following age groups: the Precambrian group, such as the White Pine deposit of Michigan (White and Wright, 1954) and the Rhodesian Copperbelt in Africa (Garlick, 1964), the Tertiary group which includes the deposit at Corocoro, Bolivia (Ljunggren and Meyer, 1964), or the Late Pennsylvanian-Permian-Early Triassic group, which includes the southwestern Oklahoma deposits. Other deposits in this last group include those of the Colorado Plateau (Soule, 1956), and the Kupferschiefer of England, Germany, and Poland (Deans, 1950).

Other representatives of this class of deposits have been found at Boleo, Baja California, Mexico (Nishihara, 1957); in England (Deans, 1950); Germany (Deans, 1950); Poland (Serkies and others, 1965); Corocoro, Bolivia (Ljunggren and Meyer, 1964); New Brunswick, Canada (McCauley, 1958); and in Oklahoma (Ham and Johnson, 1964), Kansas (Stroud and others, 1970), Pennsylvania (McCauley, 1958), and Colorado, New Mexico, and Texas (Soule, 1956) of the United States.

Although the occurrences are called "redbed type," the metals are concentrated in black, gray, green, or white shales and sandstones associated with red sandstones, shales, and conglomerates (Fischer, 1937; Soule, 1956). There is also an association of redbed copper occurrences with evaporites (Davidson, 1965; Brongersma-Sanders, 1968).

There is some evidence that the bodies of water in which copper shales were deposited were nearly filled with sediment, and that the water might not have covered some of the overlying sediment. In some examples, as in north-central and northwestern Oklahoma, laminated dolomites or mud-cracked limestones are near the stratigraphic position of the copper-bearing shales. Also, the "rote Faule" overlying the section containing the Kupferschiefer ore bed are interpreted as stream deposits.

Another characteristic of this class of heavy metal occurrences is the small number of minerals which are found and the small number of modes of occurrence. Unoxidized deposits are composed mainly of chalcocite, with bornite, chalcopyrite, native copper, cuprite, sphalerite, galena, and native silver either absent or present in minor quantities (Fischer, 1937; Deans, 1950; Brown and Trammell, 1966; Trask, 1925). Oxidized deposits are composed mainly

of malachite with subsidiary azurite, although chrysocolla has been found (Soule, 1956).

Although recognizable vegetal matter is usually absent or rare in copper shales, Trask (1925) reported that fragments of land plants had been found in the Kupferschiefer deposit. Fragments of wood are common in conglomerates and sandstones of Oklahoma. They are replaced by chalcocite or silicified and replaced by malachite or azurite.

Both horizontal and vertical zoning has been found in several redbed copper deposits. Of the deposits whose zoning patterns are mentioned in the literature, all but one, the Roan Antelope deposit in Rhodesia, are zoned upward from barren rock, successively through the greatest concentrations of copper, lead, and zinc (Fischer, 1937; Deans, 1950; Dunham, 1964). Wedepohl (1964) pointed out that this is the order of decreasing solubility of the simple sulfides of copper, lead, and zinc, and the metals were localized by a sedimentary concentration mechanism. This is the well known Schurmann's Series of metal affinity for sulfur (Park and MacDiarmid, 1964). For those few deposits which have had their stratigraphy fully worked out, we know that, with one exception, all were deposited in regressing seas (Clapham, 1970; Richter, cited by Deans,

1950). The lone exception in both vertical zoning and stratigraphy is the Roan Antelope deposit in Rhodesia, which apparently was deposited in a transgressive sedimentary package (E. N. Cameron, personal communication, 1964; Garlick, 1963).

The pattern of horizontal zoning has not been worked out for as many deposits as vertical zoning. However, the Roan Antelope deposit is exceptional again. Richter (cited in Deans, 1950) concluded that, in the Kupferschiefer, zinc was concentrated in shallow water closer to the shore than copper. Garlick (1963) interpreted the horizontal zoning at the Roan Antelope deposit to consist of seven zones, in order of increasing distance from shore, a barren zone, followed by zones of chalcocite, bornite, chalcopyrite-carrollite, galena, sphalerite, and pyrite. The Roan Antelope deposit is in rocks which are unfossiliferous with the possible exception of stromatolites (Malan, 1964; Paltridge, 1968), and the exact placement of time planes may be impossible. If indeed the placement of time planes in the Roan Antelope deposit, presumably along bedding planes, is in error due to the lack of good biostratigraphic control or the metamorphism in the district, a stratigraphic situation such as Figure 1 occurs.

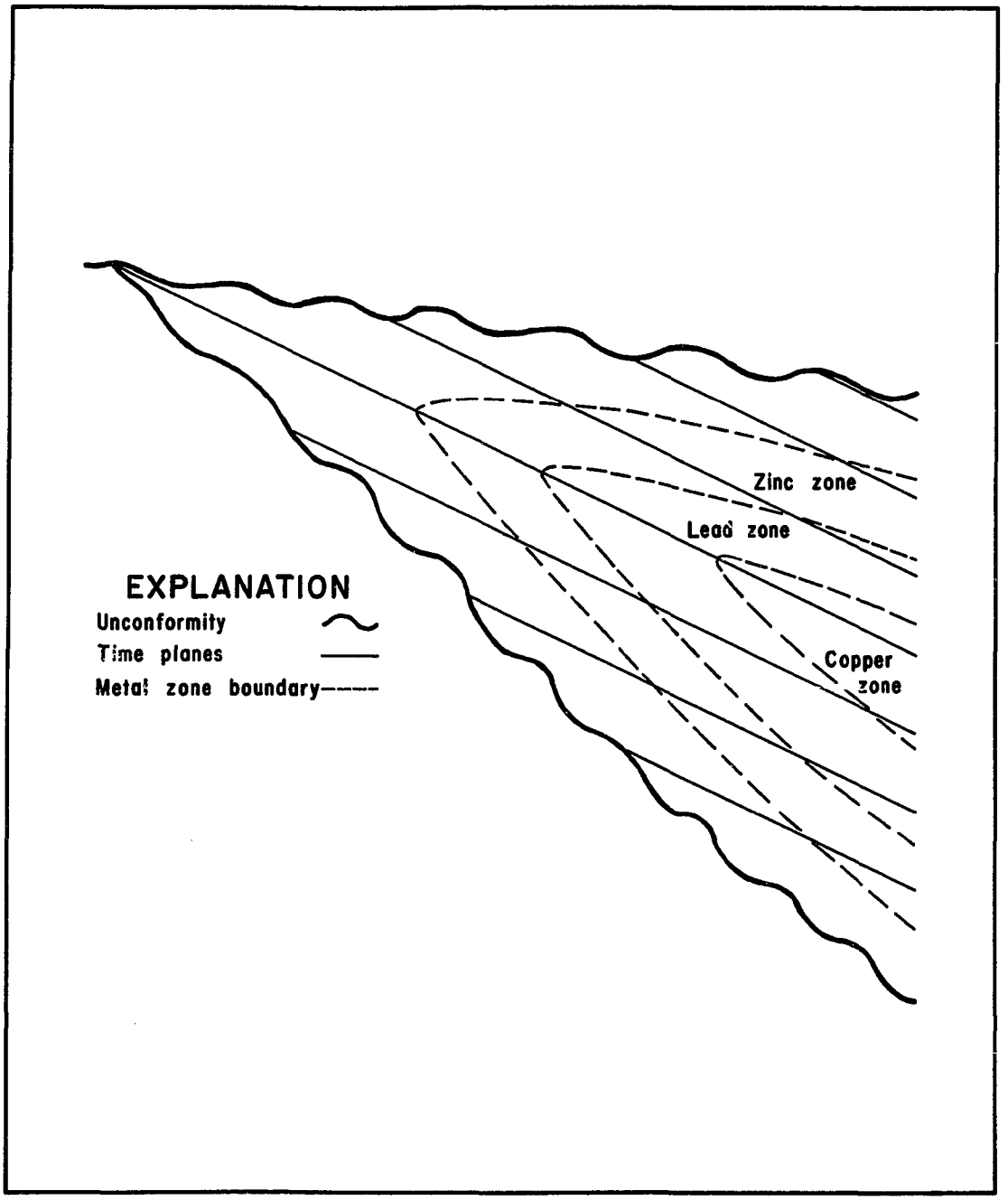

Fig. I. Relationship between metal zones (generalized), bedding, and transgressive-regressive sequences, generalized for redbed copper shale deposits worldwide. Fig. I illustrates a zoning pattern consistent with known occurrences, which might have formed by syngenetic precipitation of copper, lead, and zinc minerals. Origin of metal zones discussed in the text. (Deans, 1950, and Garlick, 1963).

Figure 1 illustrates a hypothetical relationship between metal zones and stratigraphy which is consistent with a sedimentary hypothesis of origin for redbed copper shale deposits.

It has been found that for any single hydrothermal deposit or district of sulfide ore, the range of values for $\delta\ ^{34}S/^{32}S$ is very small. Modern culture experiments on the sulfur isotope ratios of dissolved sulfate and sulfide produced by bacteriological reduction of sulfate indicate that sedimentary sulfide deposits should have a wide range of values for $\delta\ ^{34}S/^{32}S$ (Jensen and Nakai, 1964). These experiments also indicate that the sulfur isotope ratio for sulfide produced by bacteriological reduction of sulfate is always lower than the sulfur isotope ratio of the original sulfate. In only a few cases can the sulfur isotope ratios of a possible sedimentary sulfide and a possible parent sulfate be compared. The Creta deposit of southwestern Oklahoma is one of these.

Several of the class characters of redbed copper deposits are especially pertinent in the study of data from the southwestern Oklahoma deposits: the number of minerals and modes of occurrence are small, and the minerals are stable at low temperatures and low pressures; and the

pattern of zoning will be important. With these in mind, we pass to the consideration of the specific deposits of this study.

LOCATION AND GEOLOGIC SETTING OF OKLAHOMA DEPOSITS

The deposits at Creta and Mangum were selected as the topics of this dissertation because they were the only copper shale locations known in the state at the time, and they are still the only economic or potentially economic concentrations of copper known in Oklahoma sedimentary rocks. They are also much better exposed, due to the mining and prospecting work, than any other redbed copper locations in Oklahoma.

Location

The Mangum deposit is located in Greer County, south of Mangum, Oklahoma, in Ts. 3 and 4 N., R. 22 W. (Fig. 2). The deposit is about 8 miles long north-south and 2 miles wide east-west (Fig. 3).

The Creta deposit is located in Jackson County, southwest of Olustee, Oklahoma, in the western two-thirds of Ts. 1 and 2 S., R. 22 W. (Fig. 2). Information and samples are available for a rectangular area, 4 miles long

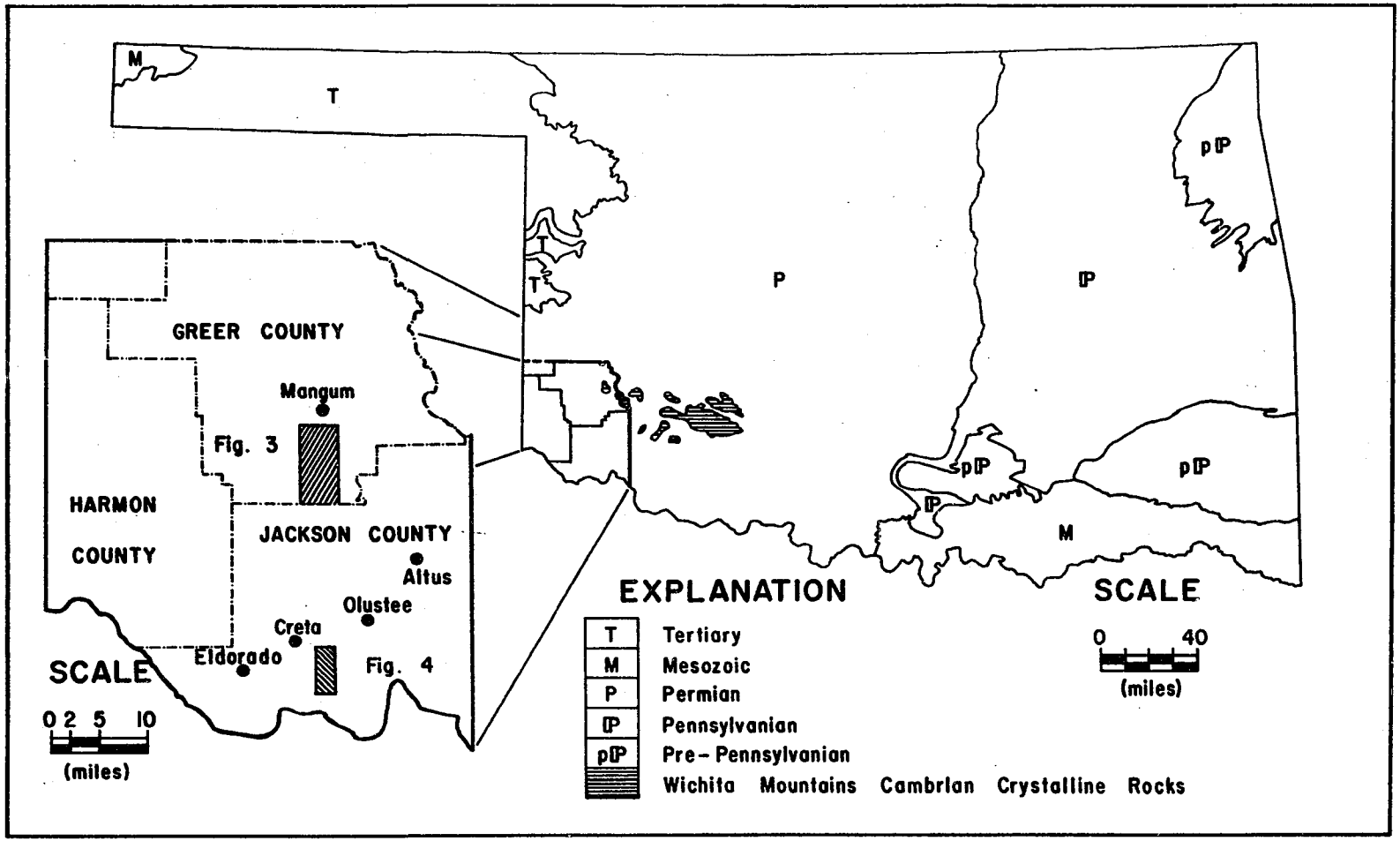

Fig. 2. Index Map of Oklahoma, (Miser and others, 1954).

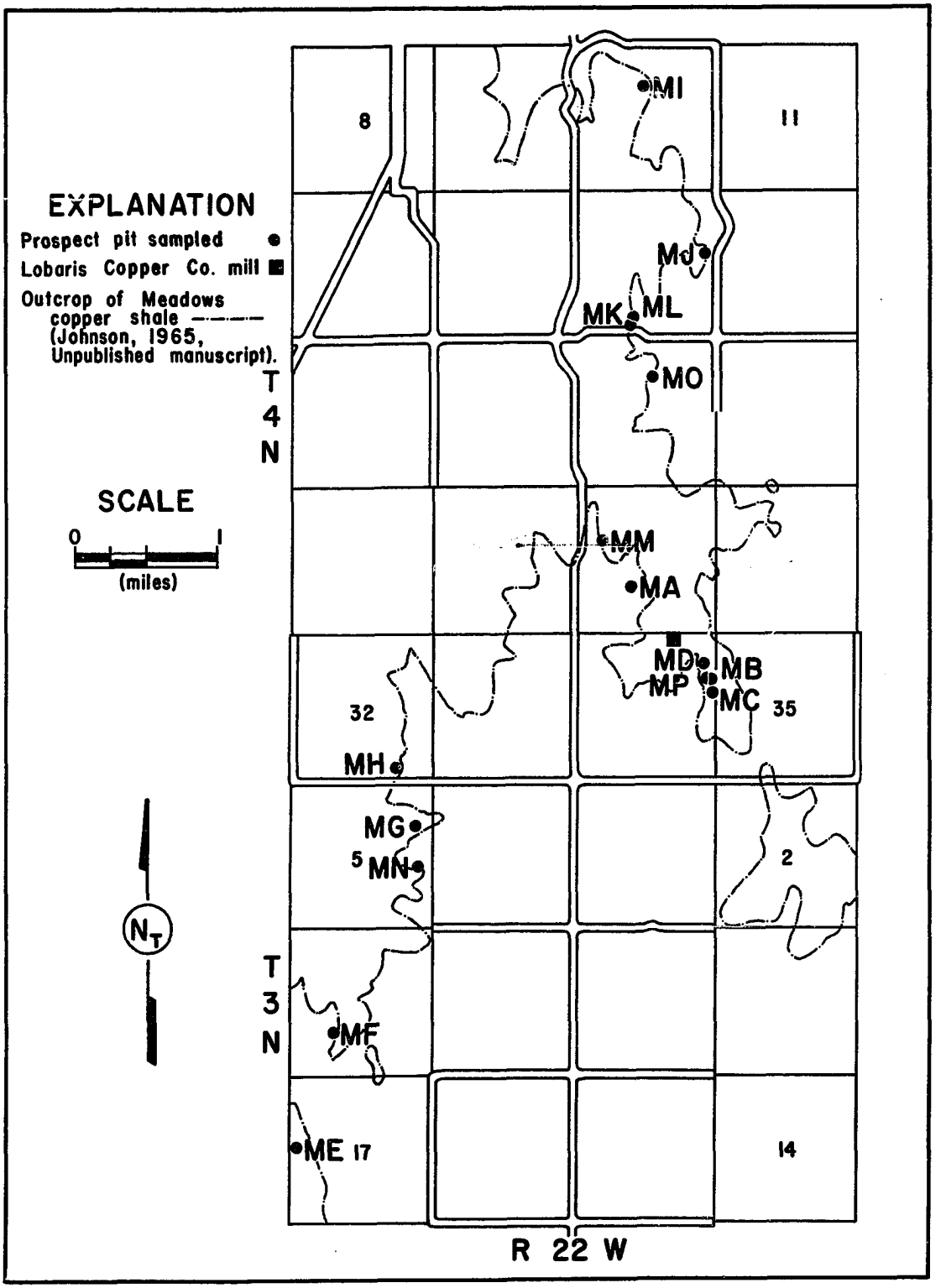

Fig. 3. Sample location map, Mangum area, Oklahoma.

north-south and 2 miles wide east-west (Fig. 4).

Stratigraphy

Both copper shale deposits are in the upper part of the Permian Flowerpot Formation in the El Reno Group. Much of the Flowerpot Shale was deposited in a marine environment, as evidenced by gypsum, dolomite, and halite interbedded with the shales (Ham and Johnson, 1964; Ward, 1963) (Fig. 5). A brackish water or shallow marine environment has been postulated (Wilson, 1962) for a bed at essentially the same stratigraphic position as the Mangum copper shale at a site several miles west of the Mangum deposit.

The copper shale at Creta has been named tentatively the "Prewitt bed," and the copper shale at Mangum has been named the "Meadows bed" (K. S. Johnson, unpublished manuscript, 1971). Both copper-bearing beds consist of laminated shale in the upper part and blocky claystone in the lower part. The Prewitt bed ranges from 6 to 16 inches thick, but in most locations it is about 8 inches thick and comprises 3 inches of laminated shale underlain by 5 inches of claystone. The Meadows bed is 0 to 20 inches thick, averaging about 11 inches thick, of which part of the bed was laminated and part was blocky.

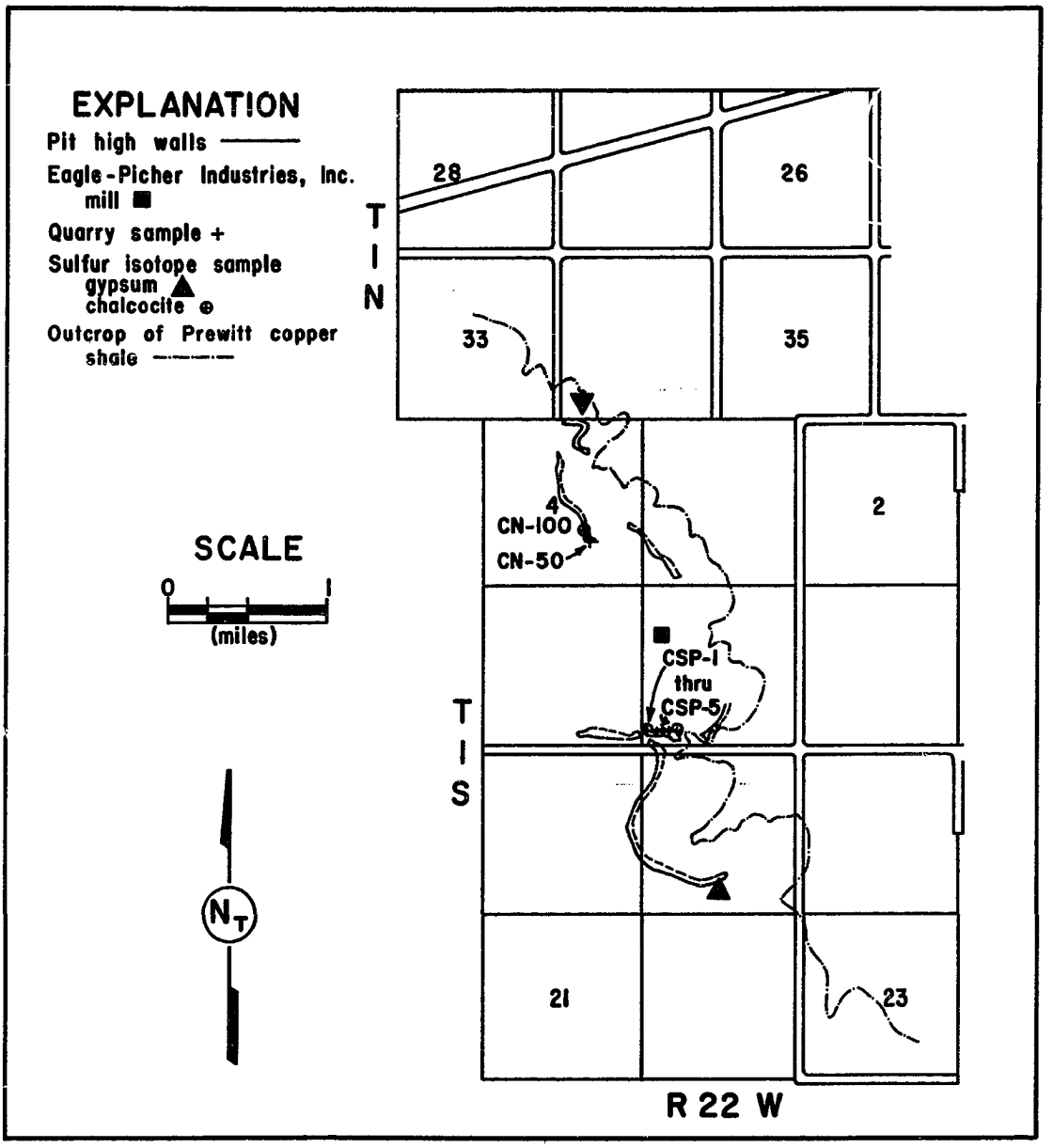

Fig. 4. Sample location map, Creta area, Oklahoma, (Ham and Johnson, 1964).

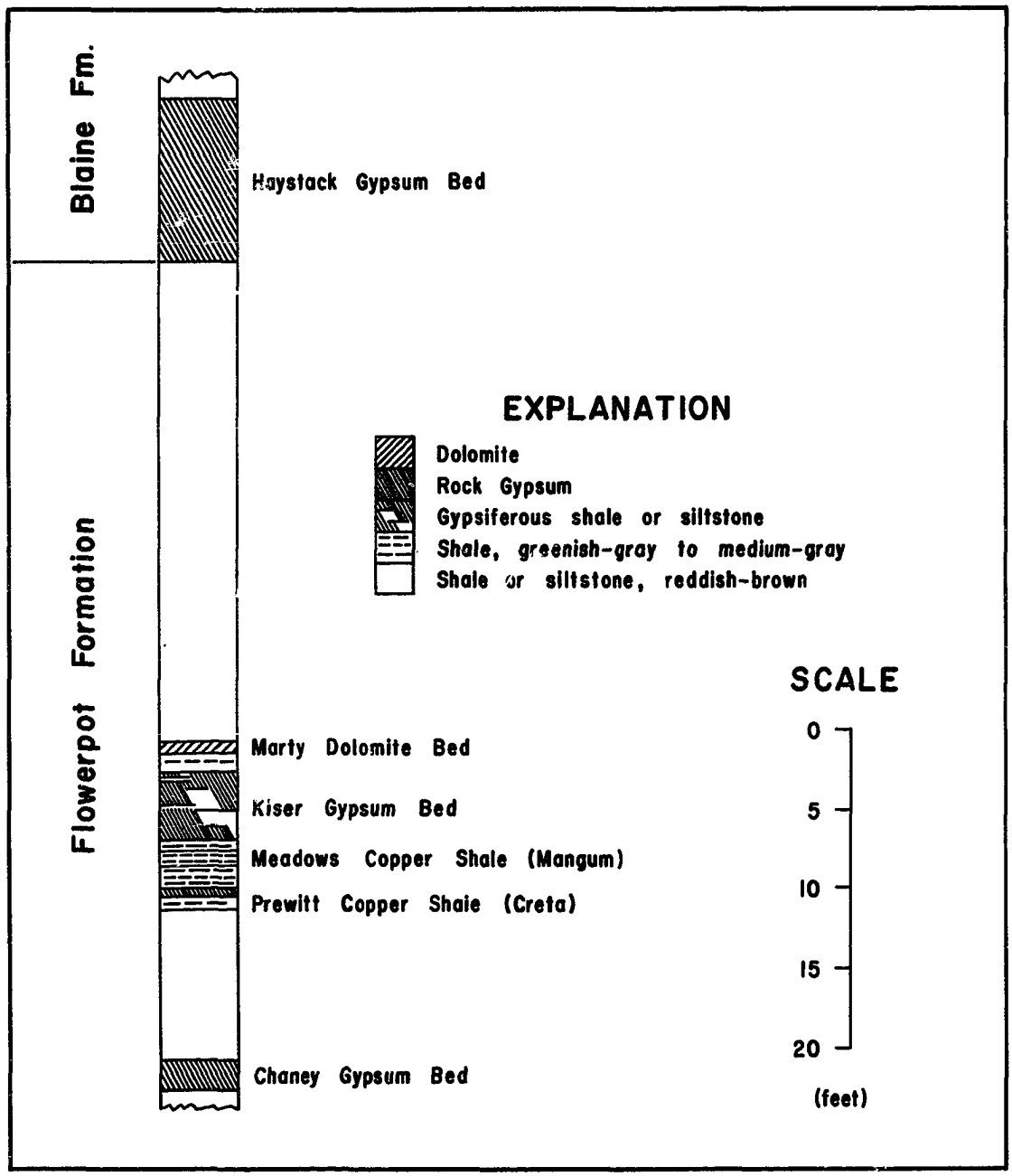

Fig. 5. Composite stratigraphic section, Flowerpot Formation, southwestern Oklahoma, (Johnson, 1971, Unpublished manuscript).

In the Creta and Mangum areas, the Kiser bed occurs a few feet above the Prewitt and Meadows copper shales (Fig. 5). It is commonly a shaly, greenish-gray gypsum. A few feet above the Kiser bed is the Marty bed, a laminated, microgranular dolomite.

Overlying the Flowerpot Formation is the Haystack Gypsum Member of the Blaine Formation. The Blaine Formation consists of gypsum beds, each 5 to 30 feet thick and normally underlain by a thin dolomite, interstratified with reddish-brown and greenish-gray shales, commonly 5 to 30 feet thick.

Structural Geology

The basement rocks under the Mangum deposit are granites of the Middle Cambrian Wichita Group. The depth to the basement is approximately 2000 to 3000 feet below ground level. Major tectonic features in the area are the Wichita uplift to the north and the Burch Fault to the southwest. The Burch Fault, a normal fault downthro. -o the south, experienced its last movements in Late Pennsylvanian-Early Permian time (Ham and others, 1964), well before deposition of the Flowerpot Formation.

The Creta deposit, on the other hand, is located on the southeast side of the Hollis Basin. The basement,

composed of the Late Precambrian or Early Cambrian Tillman Group of metasedimentary rocks, is approximately 11,000 feet below ground level (Ham and others, 1964).

No folding or faulting was observed in marker beds above or below the copper shale in either deposit, and detailed geologic mapping in both areas has failed to reveal any folds or faults.

METHODS OF INVESTIGATION

Sample Collection

Outcrop and Quarry Samples

Outcrop channel samples were collected on the cleaned faces of 16 prospect pits in the Mangum deposit (Fig. 3) and in the quarry at the Creta deposit (Fig. 4). Each lithologic interval which could be distinguished by color, the presence or absence of fissility or lamination, gypsum content, apparent copper mineral content, and sand content was independently described and sampled (Appendices I and IV).

Core Samples

Eagle-Picher Industries, Inc. gave the author one-eighth splits of 65 crushed core samples. The 65 samples represent selected intervals of the Prewitt copper shale from 13 diamond drill holes. The top sample from each diamond drill hole is the laminated upper part of the Prewitt copper shale; the lower samples are 3 inch intervals of gray, copper-bearing claystone underlying the

laminated bed.

Sample Treatment

Outcrop and Quarry Samples

All outcrop or quarry samples from both deposits were examined, and one piece large enough for thin section or polished section was removed from most samples. The remainder was crushed to approximately one-quarter inch maximum diameter, split to less than 2 ounces volume, and ground to minus-200 mesh in a Pitchford Selective Uniform Particle Size grinder. For x-ray fluorescence spectrograph analysis, 4 grams of shale powder, dried 24 hours in an oven, was hand mixed with 1 gram of 99 percent hydrolyzed polyvinyl alcohol and briquetted with a pressure of 30 tons per square inch, applied for one minute. The remainder of the powder was saved for mineralogical analysis.

Core Samples

The crushed core samples were usually under 2 ounces volume as received; these were split twice and one-fourth of each sample was ground to minus-200 mesh in the Pitchford grinder. The briquetting procedure was the same as utilized for the outcrop and quarry samples.

Chemical Analysis

X-ray Fluorescence Analysis

Analytical procedure. Samples were analyzed for CuO, ZnO, MoO_3, CaO, K_2O, Pb, Ag, U, V, Ni, Co, and total iron as Fe_2O_3 by x-ray fluorescence techniques (Table 1) using the Siemens SRS x-ray fluorescence spectrometer in the School of Geology and Geophysics. The analyses were calculated as oxides of metals or metals in their elemental states, according to the procedure used in the literature source for the standards (Table 2). Analyses of calcium and potassium oxides utilized a gas proportional counter with gas composed of 10 percent methane and 90 percent argon, flowing through the counter at 0.08 cubic feet per hour. Background and peak counts were always taken in the same order, and were not started until the sample chamber pressure reached 100 microns of mercury. A scintillation counter was used for the elements with atomic number greater than 20, and the recommendations of the X-ray Periodic Chart (General Electric, 1965) were followed.

Analytical standards. Standards were either briquettes made by previous students working on their own research, or briquettes made from ground and mixed rocks of

Table 1 Analytical Procedure for X-ray Fluorescence Analysis

Element	Cu	Pb	Zn
Counter	Scintillation Counter	Scintillation Counter	Scintillation Counter
voltage	1175	1100	1385
Collimator Slits	0.15 °2θ	0.15 °2θ	0.15 °2θ
Sample holders	Aluminum, 23 °2θ	Aluminum, 23 °2θ	Aluminum, 23 °2θ
Crystal	LiF	LiF	LiF
Primary X-rays	Tungsten, 30 KV,16 MA	Tungsten, 60 KV,20 MA	Tungsten, 30 KV,16 MA
peak	40.654, 40.250 °2θ	33.665-33.686 °2θ	41.99 °2θ
background	39.620 °2θ	34.440 °2θ	41.00 °2θ
Pulse Height Analyzer			
baseline	5.00-13.00 volts	5.00 volts	6.90 volts
window	18.00-24.00 volts	6.00 volts	20.89 volts
Attenuator	10X2	10X2	10X2
Counting time	1 minute	1 minute	1 minute

Element	Ag	Co	Ni
Counter	Scintillation Counter	Scintillation Counter	Scintillation Counter
voltage	1000 volts	1075 volts	1100 volts
Collimator Slits	0.15 °2θ	0.15 °2θ	0.15 °2θ
Sample holders	Aluminum, 23 °2θ	Aluminum, 23 °2θ	Aluminum, 23 °2θ
Crystal	LiF	LiF	LiF
Primary X-rays	Tungsten, 60 KV,20 MA	Tungsten, 30 KV,16 MA	Tungsten, 30 KV,16 MA
peak	15.634-15.761 °2θ	52.550-52.578 °2θ	48.458-48.468 °2θ
background	17.000 °2θ	54.000 °2θ	50.000 °2θ
Pulse Height Analyzer			
baseline	5.00 volts	5.00 volts	5.00 volts
window	7.00 volts	15.50 volts	8.42 volts
Attenuator	10X2	10X2	10X2
Counting time	1 minute	1 minute	1 minute

Table 1 (continued)

Element	Ca*	K*	total Fe as Fe_2O_3
Counter	Gas Proportional Counter	Gas Proportional Counter	Scintillation Counter
voltage	2010 volts	2100 volts	1300 1175 1250
Collimator Slits	0.15 °2θ	0.15 °2θ	0.15 °2θ
Sample holders	Aluminum, 23 °2θ	Aluminum, 23 °2θ	Aluminum, 23 °2θ
Crystal	PET	PET	LiF
Primary X-rays	Chromium, 20 KV, 20 MA	Chromium, 20 KV, 20 MA	Tungsten, 20 KV, 30 MA
peak	41.272-41.296 °2θ	50.563-50.606 °2θ	51.546-52.500 °2θ
background	40.062 °2θ	48.750 °2θ	53.000 °2θ
Pulse Height Analyzer			
baseline	8.17 volts	14.00 volts	5.00,4.60,10.0,16.5
window	8.73, 10.42 volts	16.00 volts	12.55,12.55,18.0,16.5
Attenuator	10X2	10X2	10X2
Counting time	1 minute	1 minute	1 minute

Element	Mo	U	V
Counter	Scintillation Counter	Scintillation Counter	Scintillation Counter
voltage	1000 volts	1050 volts	1000 volts
Collimator slits	0.15 °2θ	0.15 °2θ	0.15 °2θ
Sample holders	Aluminum, 23 °2θ	Aluminum, 23 °2θ	Aluminum, 23 °2θ
Crystal	Topaz	LiF	LiF
Primary X-rays	Tungsten, 50 KV,50MA	Tungsten, 50 KV,10 MA	Tungsten, 60 KV,20MA
peak	30.254, 30.288 °2θ	26.002-26.038 °2θ	15.634-15.758 °2θ
background	29.680 °2θ	24.250 °2θ	17.000 °2θ
Pulse Height Analyzer			
baseline	7.86 volts	7.50, 7.00, 8.46 volts	5.00 volts
window	7.10 volts	19.0, 14.5, 13.81 volts	7.00 volts
Attenuator	10X1	10X1	10X2
Counting time	1 minute	1 minute	1 minute

* 100 micron vacuum, 6 micron anodized Mylar foil

Table 2

Chemical Standards

Copper	Briquettes of Goose Lake Illite with 0.00, 0.5, 1.0, 1.5, 2.0, 2.5, 4.0, 5.0, 6.0, and 7.11 weight percent of CuO added.
Zinc	Briquettes of Goose Lake Illite with 0.00, 0.25, 0.50, and 1.00 weight percent ZnO added.
Molybdenum	Briquettes of Goose Lake Illite with 0.00, 0.25, 0.50, and 1.00 weight percent MoO_3 added.
Uranium	Briquettes containing 0.10, 0.25, 0.50, and 1.00 weight percent U, from the set of standards owned by the School of Geology and Geophysics, University of Oklahoma.
Silver	Briquettes containing 0.7, 22.2, 42.2, and 257 ppm Ag, from the set of standards owned by the School of Geology and Geophysics, University of Oklahoma.

Table 2 (continued)

Iron		
GA	2.81 weight percent Fe_2O_3	Roubalt and others, 1966
T-1	6.03 weight percent Fe_2O_3	Thomas, 1963
QMC I-1	0.61 weight percent Fe_2O_3	Poole, 1968
AMC M-2	9.40 weight percent Fe_2O_3	Poole, 1968
AGV-1	6.78 weight percent Fe_2O_3	Flanagan, 1969
Cobalt		
DTS-1	132 ppm Co	Flanagan, 1969
PCC-1	112 ppm Co	Flanagan, 1969
W-1	50 ppm Co	Fleischer, 1969
AGV-1	15.5 ppm Co	Flanagan, 1969
Nickel		
T-1	12 ppm Ni	Kaye, 1965
NBS-98	50 ppm Ni	Kaye, 1965
Vanadium		
BCR-1	384 ppm V	Flanagan, 1969
DTS-1	19 ppm V	Flanagan, 1969
Lead		
GSP-1	52.4 ppm Pb	Flanagan, 1969
AGV-1	35.4 ppm Pb	Flanagan, 1969
PCC-1	13.3 ppm Pb	Flanagan, 1969
Calcium		
AGV-1	4.98 weight percent CaO	Flanagan, 1969
W-1	10.95 weight percent CaO	
GA	2.48 weight percent CaO	Roubalt and others, 1966
QMC I-1	0.84 weight percent CaO	Poole, 1968
G-2	1.96 weight percent CaO	
Potassium		
AGV-1	2.89 weight percent K_2O	Flanagan, 1969
BCR-1	1.68 weight percent K_2O	Flanagan, 1969
DTS-1	0.02 weight percent K_2O	Flanagan, 1969
GSP-1	5.48 weight percent K_2O	Flanagan, 1969
W-1	0.70 weight percent K_2O	
T-1	1.23 weight percent K_2O	

various composition which had been originally employed to test analytical precision in various laboratories (Table 2).

Analytical reproducibility. Reproducibility was estimated for the x-ray fluorescence analyses by repeated analysis of some specimens. Commonly, 10 percent of the specimens were reanalyzed. Values of analytical reproducibility for given ranges of composition are given in Table 3.

Wet Method of Analysis for Organic Matter

Approximately 2 grams of minus-200 mesh powder of the shale samples was weighed into a 250 ml. beaker and covered with 10 ml distilled water. Then 10 ml of 30 percent hydrogen peroxide was added and the slurry was digested at 80° Centigrade. After digestion, another 5 ml of 30 percent hydrogen peroxide was added and digestion continued. When digestion was complete, the beakers were transferred to an oven where the ground shale was dried at the same temperature at which it had been dried prior to the first weighing. The weight loss is assumed to represent the original weight of organic matter oxidized by the large excess of H_2O_2 and evolved during digestion. This method is a modification of one described by Jackson (1958) and was chosen to avoid the dehydration of clay minerals at elevated temperatures.

Table 3 Reproducibility of Chemical Analyses

Element	Reproducibility	Maximum Range of Composition
Copper	Few analyses repeated	0.11-6.64 % CuO
Zinc	Maximum error 0.002 % ZnO (10)	0.008-0.045 %
Molybdenum	Maximum error 0.003 % MoO_3 (23)	0.004-0.014 %
Uranium	Maximum error 0.001 % U (23)	0.002-0.013 %
Silver	Maximum error 8 ppm Ag (24)	0-92 ppm
Iron	Few analyses repeated	0.56-10.17 % Fe_2O_3
Cobalt	Maximum error 4 ppm Co (23)	0-66 ppm
Nickel	Maximum error 10 ppm Ni (26)	0-72 ppm
Vanadium	Maximum error 24 ppm V (26)	0-193 ppm
Lead	Maximum error 26 ppm Pb (26)	3-391 ppm
Calcium	Few analyses repeated	0.33-14.85 % CaO
Potassium	Few analyses repeated	0.51-5.01 % K_2O
Organic matter	Maximum error 0.54 weight % organic matter	0.01-6.64 %

() indicates number of analyses repeated.

Mineralogical Analysis

Because considerable time elapsed between grinding of all of the shale samples and analysis of the specimens for gypsum, there was enough time for much of the gypsum in the specimens to invert to bassanite, the calcium sulfate hemihydrate better known as "Plaster of Paris." It is certain that time and humidity conditions in the laboratory made this transformation possible at ordinary temperatures, because one set of gypsum standards contained gypsum the first four times they were x-rayed and bassanite on the fifth run. This transformation made it necessary to do gypsum and bassanite analyses, recalculating the bassanite concentrations to weight percent gypsum.

Gypsum, bassanite, and quartz content in unknowns were all measured by scanning slowly across a back-filled powder pack, and then comparing the area of the particular peak with a working curve set up from similar measurements on standards made with known amounts of gypsum, bassanite, or quartz added.

All mineral analyses were adjusted to total 100 percent in the following manner: copper minerals and illite were calculated from CuO and K_2O contents, respectively, and rounded to whole percents, gypsum was accepted directly

from analysis up to the maximum gypsum content allowable on the basis of the CaO analysis, quartz was accepted directly from analysis, and chlorite was found by the method of differences.

Gypsum-Bassanite

Analytical procedure. Minus-200 mesh powder of each shale sample was packed in a standard aluminum powder pack and placed in the Siemens x-ray diffractometer. Specimens were exposed during a goniometer rotation of 1.0 to 1.3 $^{\circ}2\theta$ with the 10 centimeter per minute chart speed. The 3.06 Å peak of gypsum and the 3.00 Å peak of bassanite were measured for each standard and unknown by graphically estimating the background, and then measuring the area of the peak with a Dietzgen planimeter. The areas of the peaks for shale samples whose gypsum and bassanite contents were unknown were compared to a working curve made from the peak areas of a low calcium sample with known amounts of gypsum and bassanite. Some samples were rotated and the several peaks were measured in order to reduce the effects of induced orientation in unknowns.

Analytical standards. The standards for this part of the research consisted of known amounts of minus-200

mesh gypsum or bassanite (commercial Plaster of Paris) hand-mixed with known amounts of a shale, also ground to minus-200 mesh. The gypsum used in standards compared with Creta specimens was collected at Creta; gypsum was collected at Mangum for runs on Mangum specimens. Standard curves were least-squares if linear, and hand-drawn if curved.

Analytical accuracy and reproducibility. Accuracy was tested by analyzing mixtures made up by another student secretly; reproducibility was tested by reanalyzing these. The accuracy is dependent on the amount present, but is about ± 5 percent of the specimen. Reproducibility was also about ± 5 percent of the specimen. Therefore, accuracy is as good as precision will allow.

Quartz

Analytical procedure. The procedure was generally the same for quartz as it was for gypsum and bassanite. The 3.34 Å peak was used to estimate the quartz content of each specimen.

Analytical standards. The standard quartz added in known amounts to a ground shale from Mangum and one from Creta for quartz analyses was a rock crystal quartz from the School of Geology and Geophysics mineralogy storeroom,

ground to pass a 200 mesh screen. Because the shale bases could not be selected for very low initial quartz content as they had been for very low gypsum-bassanite content, the standards were run, and then extrapolated back to the point of zero quartz, zero peak area.

Analytical accuracy and reproducibility. These were evaluated in the same manner as for gypsum and bassanite, and both accuracy and reproducibility are about 5 percent of the specimen.

Chalcocite-Malachite

The amount of chalcocite or malachite present is calculated from the weight percent CuO, by conversion to weight percent Cu, and multiplying this by the ratio of the formula weight of chalcocite or malachite to formula weight of copper. No other copper minerals were detected during either x-ray analysis or hand specimen examination.

Illite-Chlorite

Because the only clay minerals found in either deposit were illite and chlorite, all specimens were assumed to contain only illite and chlorite clay minerals. The weight percent illite was calculated from the weight percent K_2O, using analysis 18 in the table of illite analyses in

Deer, Howie, and Zussman (1962) as a model. Chlorite content of all specimens was arrived at by the method of differences.

Sulfur Isotope Analysis

Sample Preparation

Seven samples of Prewitt copper shale, selected to give good vertical and areal distribution in the Creta deposit, were oven dried, immersed in kerosene, and then submerged in hot water. Subsequent minor stirring and ultrasonic treatment were sufficient to completely break down the samples. The clay minerals were decanted, and saved for x-ray diffraction. The chalcocite in the remainder (primarily quartz, chalcocite, and some gypsum) was separated from quartz and gypsum by settling in tetrabromoethane. The sulfide-rich heavy fraction of each sample was x-rayed, pulverized in an agate mortar, and resettled in tetrabromoethane, before it was sent to the University of Utah Laboratory of Isotope Geology.

Two samples of the gypsum bed immediately above the Prewitt copper shale at Creta were collected (Figs. 4 and 5). Portions of the bottom-most laminated gypsum of each sample were pulverized, and after examination showed that there were

no contaminating satinspar veinlets, these samples were also sent to the Laboratory of Isotope Geology of the University of Utah.

Results

Samples L-16 and L-17, the southern and northern gypsum samples (Fig. 4) respectively, had $\delta^{34}S/^{32}S$ values of +4.67 and +6.25. The values of $\delta^{34}S/^{32}S$ for the chalcocite concentrates are below (Table 4).

Table 4

Results of Sulfur Isotope Analysis of Chalcocite Concentrates

CN-100	(54.75-60.75)	-34.59
CSP-1	(56.00-62.00)	-19.17
CSP-1	(62.00-67.50)	- 0.86
CSP-5	(60.75-76.25)	-26.77
B	(4.10- 7.10)	-19.07
C	(1.20- 4.20)	-29.72
D	(3.00- 6.00)	-30.27

Computer Methods

The computer was used to calculate correlation coefficients for each pair of analytical variables, treating each deposit separately. Then the samples were organized into classes by color of shale, with one additional group including those gray shales whose copper contents exceeded

the average for the deposit.

Eighteen observations were obtained for each of 108 Mangum samples (Appendices 2, 3) and 118 Creta samples (Appendices 5, 6). The data for each area were run separately on program BMD03D of the Biomedical set of programs from the UCLA Health Sciences Computing Facility. The output consisted of the mean and standard deviation for each variable, and a matrix of linear correlation coefficients for each area (Tables 5, 6, and 9). Following the run to establish correlation coefficients for each deposit, the input cards for each deposit were grouped into color coded groupings and a group containing specimens whose copper content was above the average of all specimens in that deposit (Tables 7, 8, 10 and 11).

Subsequent statistical work on each observation or pair of observations included (1) determining which correlation coefficients are different in the 2 deposits for a significance level of 95 percent (Ostle, 1967), (2) testing the equality of variance of each observation for the group of shales in each deposit (significance level 90 percent Mangum, 98 percent Creta) and (3) for a significance of 95 percent, testing the hypothesis that means of observations are identical for all pairs of shale groups.

Table 5

Means and Standard Deviations of Variables,
Mangum and Creta

MANGUM

Variable		Mean	Standard Deviation
Quartz	(%)	26.16	6.29
Gypsum	(%)	14.46	14.28
Illite	(%)	46.72	10.21
Chlorite	(%)	11.62	10.31
Malachite	(%)	1.18	1.92
Ag	(ppm)	32.9	12.2
Pb	(ppm)	41.9	47.8
V	(ppm)	118.1	36.9
Co	(ppm)	18.8	11.0
Ni	(ppm)	48.2	14.2
CuO	(%)	0.92	1.32
total iron as Fe_2O_3	(%)	5.49	1.45
K_2O	(%)	3.63	0.79
CaO	(%)	5.06	3.63
Organic Matter	(%)	1.62	0.79
ZnO	(%)	0.036	0.005
U	(%)	0.009	0.001
MoO_3	(%)	0.011	0.002

CRETA

Variable		Mean	Standard Deviation
Quartz	(%)	25.42	11.21
Gypsum	(%)	11.33	20.07
Illite	(%)	50.88	11.84
Chlorite	(%)	11.81	10.52
Chalcocite	(%)	0.44	0.81
Ag	(ppm)	40.0	19.0
Pb	(ppm)	50.3	62.2
V	(ppm)	111.7	39.8
Co	(ppm)	19.7	11.0

Table 5 (continued)

Variable		Mean	Standard Deviation
Ni	(ppm)	46.6	13.6
CuO	(%)	1.11	1.54
total iron as Fe_2O_3	(%)	5.23	1.76
K_2O	(%)	3.95	0.92
CaO	(%)	2.94	2.90
Organic Matter	(%)	1.50	0.76
ZnO	(%)	0.030	0.009
U	(%)	0.009	0.002
MoO_3	(%)	0.009	0.002

Gypsum	Illite	Chlorite	Malachite	Ag	Pb	V	Co	Ni	CuO	Fe_2O_3	K_2O	CaO	Organic Matter	ZnO	U	MoO_3	
-.41	.31	-.34	-.07	.36	0.0	.41	.29	.35	-.06	.34	.31	-.19	-.06	.19	.08	.19	Quartz
	-.70	-.39	0.0	-.53	-.14	-.65	-.51	-.68	.02	-.60	-.70	.77	-.27	-.49	-.01	-.29	Gypsum
		-.24	.04	.55	.06	.89	.59	.91	.02	.80	1.0	-.91	.28	.63	.05	.29	Illite
			-.19	.02	.06	-.24	-.09	-.23	-.20	-.16	-.24	0.0	-.03	-.02	.01	.03	Chlorite
				-.32	.36	-.01	.05	.21	.98	-.23	.04	0.0	.13	-.25	-.45	-.14	Malachite
					.11	.53	.37	.57	-.34	.39	.55	-.48	.20	.49	.06	.23	Ag
						.12	.64	.24	.39	0.0	.06	-.04	-.01	0.0	-.84	-.06	Pb
							.63	.82	-.02	.76	.89	-.82	.18	.58	.01	.32	V
								.61	.08	.65	.60	-.47	.08	.41	-.50	.12	Co
									.20	.63	.91	-.85	.34	.56	-.08	.22	Ni
										-.22	.02	.02	.14	-.28	-.49	-.13	CuO
											.80	-.65	.22	.64	.06	.23	Fe_2O_3
												-.91	.29	.63	.05	.30	K_2O
													-.39	-.55	-.12	-.09	CaO
														.25	.06	-.14	Organic Matter
															.14	.14	ZnO
																.11	U

Table 6

Correlation Coefficients for Entire Mangum Deposit

Table 7 Composition Means and Standard Deviations (In Parentheses) by Shale Type, Mangum

	Mottled shales	Copper-rich shales	Gray shales	Red shales	Maroon shales
Quartz	26.4 (7.6)	26.0 (5.0)	26.2 (6.0)	26.9 (7.2)	23.6 (5.5)
Gypsum	18.4 (19.3)	13.2 (12.1)	13.0 (11.9)	16.3 (14.2)	17.4 (24.8)
Illite	44.6 (11.4)	48.5 (6.7)	47.9 (9.4)	43.6 (11.0)	45.7 (13.5)
Chlorite	11.2 (8.7)	8.8 (5.7)	11.2 (10.3)	12.4 (11.0)	14.9 (13.1)
Malachite	0.0 (0.0)	3.6 (2.3)	1.7 (2.1)	0.1 (0.5)	0.0 (0.0)
Ag ppm	30.9 (10.2)	31.0 (14.9)	34.7 (12.5)	25.9 (11.3)	33.1 (9.7)
Pb ppm	23.5 (8.0)	87.8 (71.0)	52.0 (55.8)	21.1 (6.6)	19.3 (6.2)
V ppm	124.9 (40.4)	124.0 (32.7)	119.3 (35.8)	107.3 (34.3)	115.0 (50.6)
Co ppm	17.7 (10.8)	24.0 (14.8)	19.1 (11.5)	18.6 (9.7)	18.0 (11.1)
Ni ppm	44.7 (16.9)	55.3 (9.6)	51.2 (12.8)	38.5 (12.3)	44.4 (17.2)
CuO	0.19 (0.04)	2.59 (1.61)	1.29 (1.49)	0.18 (0.09)	0.19 (0.05)
Fe_2O_3	5.66 (1.35)	5.17 (0.99)	5.21 (1.25)	6.44 (1.73)	6.06 (2.16)
K_2O	3.46 (0.89)	3.77 (0.52)	3.72 (0.73)	3.38 (0.85)	3.55 (1.04)
CaO	5.62 (3.58)	4.74 (2.97)	4.77 (3.42)	6.92 (4.59)	2.58 (1.40)
Organic matter	1.22 (0.57)	1.75 (0.48)	1.71 (0.88)	1.69 (0.41)	1.45 (0.35)
ZnO	.035 (.005)	.035 (.005)	.036 (.005)	.037 (.003)	.038 (.004)
U	.010 (.001)	.008 (.002)	.009 (.002)	.009 (.001)	.009 (.001)
MoO_3	.012 (.002)	.010 (.002)	.011 (.002)	.010 (.002)	.009 (.002)

All values weight percent unless otherwise noted.

Gypsum	Illite	Chlorite	Malachite	Ag	Pb	V	Co	Ni
						.53		.52
-.88-.58	.66			.66	.51	.54 .53	.74	.75
	-.64-.88	-.60		-.54-.51		-.60-.87	-.51	-.64-.81
	-.72			-.50	-.61	-.75	-.73	-.72
	-.66-.90	-.53-.69		-.79-.65	-.69	-.63-.80	-.72	-.74-.85
				.67	.64	.87 .95	.66	.91 .95
				.55	.71	.94	.90	.90
		.57		.85 .61	.73	.93 .78	.98	.98 .86
				.60			.53	.62
				-.54				
					.58			
				-.72				
								.77
						.54		.64
					.81	.88 .56	.79	.88 .69
							.75	.57
						.69	.69	.68
						.68	.70 .83	.75
							.54	.82 .92
							.95	.88
							.87	.94 .65
								.58 .65
								.80
								.96

Table 8

Significant Correlation Coefficients by Shale Type, Mangum

Absolute values less than 0.50 are omitted.

Key to Correlation Coefficients

r-gray shales	r-red shales
r-mottled shales	
r-maroon shales	r-Cu>avg.

CuO	Fe_2O_3	K_2O	CaO	Organic Matter	ZnO	U	MoO_3	
	.51 .71	.65	-.63 .78		.54 .52			Quartz
-.50	-.69 .74 -.59 -.68-.89	-.64-.88 -.73 -.66-.90	.78 .75 .75 1.0 .93		-.61 -.70 -.54-.76	-.59 .58	-.76 -.50	Gypsum
.63	.93-.86 .83 .98 .89		-.92-.88 -.91 -.88-.90	.73	.70 .85 .97 .76		.64	Illite
	.71	.59	-.98		.68	.58 .81		Chlorite
								Malachite
-.55 -.74	.55 .83 .77	.67 .57 .86 .63	-.72 -.64 -.68 -.60		.61 .81 .71		.59 .68	Ag
.56	.57 .58 .70	.64 .71 .74	-.59		.57 .69 .63	-.87 -.90	.55	Pb
.62	.83 .88 .87 .86 .75	.87 .95 .94 .93 .78	-.80-.89 -.95 -.75-.79	.53	.64 .87 .89 .56		.64	V
	.60 .75 .94 .99 .64	.67 .80 .98	-.91	.61	.89 .94	-.58 -.68		Co
.66	.85 .83 .66 .94 .87	.91 .95 .90 .98 .87	-.85 -.94 -.92 -.85		.68 .82 .90 .83	.58	.59	Ni
	.52	.62	-.56	.54	-.50			CuO
		.94 .86 .83 .98 .90	-.90 -.63 -.77 -.90	.73	.75 .78 .97 .85	-.55		Fe_2O_3
			-.92 -.87 -.91 -.89 -.90	.73	.71 .85 .97 .77		.65	K_2O
				-.50	-.65 -.86 -.82-.79	-.62 -.71		CaO
						.62		Organic Matter
								ZnO
								U

Gypsum	Illite	Chlorite	Chalcocite	Ag	Pb	V	Co	Ni	CuO	Fe_2O_3	K_2O	CaO	Organic Matter	ZnO	U	MoO_3	
-.71	.63	-.39	-.28	.66	-.31	.69	.25	.59	-.30	.52	.63	-.49	.01	.04	.59	.48	Quartz
	-.85	-.20	.12	-.66	.06	-.76	-.55	-.78	.15	-.75	-.85	.83	-.16	.32	-.36	-.45	Gypsum
		-.18	-.08	.66	-.24	.81	.53	.90	-.12	.83	1.0	-.84	.32	.50	.47	.42	Illite
			.08	-.16	.45	-.24	.19	-.17	.11	-.05	-.18	.31	-.17	.01	-.42	-.10	Chlorite
				-.46	.35	-.19	-.03	.13	.97	-.27	-.09	.51	-.10	-.11	-.61	-.29	Chalcocite
					-.06	.70	.48	.64	-.49	.56	.66	-.58	.20	.23	.50	.65	Ag
						-.26	.44	.05	.36	-.23	-.24	.33	-.33	-.11	-.77	.06	Pb
							.45	.78	-.20	.75	.87	-.71	.31	.37	.49	.45	V
								.61	-.07	.63	.53	-.26	.08	.45	-.02	.24	Co
									.09	.64	.90	-.54	.19	.44	.26	.42	Ni
										-.31	-.13	.47	-.11	-.13	-.65	-.31	CuO
											.83	-.59	.26	.57	.45	.26	Fe_2O_3
												-.84	.33	.50	.47	.42	K_2O
													-.32	-.21	-.53	-.40	CaO
														.26	.21	.04	Organic Matter
															.22	-.15	ZnO
																.24	U

Table 9

Correlation Coefficients for Entire Creta Deposit

Table 10 Composition Means and Standard Deviations (In Parentheses) by Shale Type, Creta

	Gypsums	Copper-rich shales	Gray shales	Red shales	Maroon shales
Quartz	1.0 (0.00)	19.2 (8.3)	25.7 (10.8)	24.7 (2.1)	29.8 (9.9)
Gypsum	90.0 (3.00)	15.7 (16.0)	10.2 (16.5)	5.0 (4.0)	1.6 (1.0)
Illite	9.0 (3.00)	47.9 (10.8)	51.6 (10.2)	47.3 (5.1)	56.4 (5.5)
Chlorite	0.0 (0.00)	15.7 (15.4)	11.8 (10.9)	23.0 (9.2)	12.0 (4.7)
Chalcocite	0.00 (0.00)	3.0 (1.56)	1.0 (1.6)	0.0 (0.0)	0.0 (0.0)
Ag ppm	1.3 (2.3)	26.0 (17.1)	41.5 (19.0)	23.0 (2.6)	41.5 (5.7)
Pb ppm	23.0 (33.8)	97.1 (82.2)	55.5 (65.6)	28.0 (4.6)	16.5 (2.9)
V ppm	2.0 (3.5)	93.9 (35.2)	113.0 (37.4)	106.0 (24.1)	130.9 (20.5)
Co ppm	0.3 (0.6)	19.6 (14.0)	19.5 (10.8)	30.7 (6.0)	24.7 (6.9)
Ni ppm	1.0 (1.0)	48.0 (13.8)	48.5 (11.9)	31.7 (9.5)	45.8 (4.7)
CuO	0.27 (0.15)	3.17 (1.56)	1.26 (1.61)	0.16 (.01)	0.15 (0.02)
Fe_2O_3	0.68 (0.18)	4.30 (1.30)	5.04 (1.38)	9.30 (0.91)	7.10 (1.34)
K_2O	0.70 (0.20)	3.71 (0.84)	4.01 (0.79)	3.68 (0.39)	4.38 (0.44)
CaO	nd	5.34 (3.85)	3.06 (2.95)	4.82 (4.46)	1.48 (1.24)
Organic matter	1.06 (nd)	1.29 (0.78)	1.48 (0.75)	0.99 (0.50)	1.83 (0.83)
ZnO	.021 (.012)	.028 (.008)	.029 (.009)	.037 (.001)	.037 (.010)
U	.008 (.002)	.007 (.002)	.009 (.002)	.009 (.001)	.010 (.001)
MoO_3	.006 (.003)	.009 (.002)	.010 (.002)	.007 (.001)	.009 (.001)

nd = not determined. All values weight percent unless otherwise noted.

Gypsum	Illite	Chlorite	Chalcocite	Ag	Pb	V	Co	Ni
-.70 -.53-.62	-1.0 .63 1.0 -.94 .88	 -.89 -.87-.52		.66	 -.58	.68 .86	 .98 -.84	.59 .83 -.76 .87
	-.78 .52 -.60	 -.65		-.65 -.76	 .65	-.87-.71 1.0	-.87-.50 -.59	1.0 -.73 .74 .55 -.70
		 -.91 .68 -.58		.62	 -.53 -.57	.87 .85 .84	.87 .99 .87	-1.0 .89 .86 .92
					 .54	 -.60 -.58	-.50 -.96 .69	 -1.0
				-.56				 .54
					1.0 -.99	-.50 .68 -.80	 .71	 .57
						 .71	.51 .77	
							1.0	-.87 .77 .69 .84
								-.87 .65 .92 .66 .59

Table 11

Significant Correlation Coefficients by Shale Type, Creta

Absolute values less than 0.50 are omitted.

Key to Correlation Coefficients

r-gypsums	r-gray shales
r-red shales	
r-maroon shales	r-Cu>avg.

CuO	Fe_2O_3	K_2O	CaO	Organic Matter	ZnO	U	MoO_3	
-.69	.60 .94 -.81 .88	.64 1.0 -.95 .88	-.57 -.78 -.80	-.95	-.84 .63	.61 .96 .62	-.69	Quartz
-.87	-.90-.78 .56 -.69	-.99-.78 .54 -.60				.50	-.87	Gypsum
-.73	.90 .95 .96 .94		-.85 -.81 -.93	-.94 .69	.51 .64	.52 .97	-.73	Illite
.95	-.99 .65	-.90 .69 -.58	.98 -.52	.72 -.62	.56	-.98	.94	Chlorite
			.52			-.62		Chalcocite
1.0-.59	.70 .66	.63	-.61	-.70 -.77	-1.0 .51	-.94 .53	.92 .63 .65	Ag
1.0		-.57		.79	-1.0	-.95-.77 -.72		Pb
-.53 -.83	1.0 .83 .85	.92 .85 .84	-.73 -.75 -.77			.52	-.83	V
-.53 -.81	1.0 .56 .99 .69 .61	.92 .99 .89	-.88 -.80	-.88	.79	1.0 -.76	-.81 .58	Co
-.98	-.90 .84 .97 .67 .95	-.99 .88 .84 .84 .92	-.59 -1.0 -.85-.90	-.63 .52	.53 .80 .59	.95 -.69	-.98	Ni
	-.90	-.70	.99		-.99	-.93-.65 -.87	.90 1.0 .83	CuO
		.95 .95 .94 .82 .94	-.81 -.95 -.75 -.93	-.80 -.54	.52 .80 .55	.52 1.0 -.74	-.90	Fe_2O_3
			-.86 -.79 -.88 -.94	-.95 .70	.51 .92 .64	.53 .96 -.78	-.70	K_2O
				.56	-.96-.52	-.54 -.92 .71	.99	CaO
					.75	-.83 -.65 .68		Organic Matter
						.97 -.67	-.95	ZnO
							-1.0 -.87	U

RESULTS

The following discussion of results and hypotheses will be based on relations between variables, as expressed by correlation coefficients, mean variables, and standard deviations of the means for the variables.

Because program BMD03D does not provide for inputting accuracy and reproducibility for each variable, all correlation coefficients have numerical values higher than real. There is no way to estimate the amount of change this problem causes. I have attempted to diminish the effect by ignoring correlation coefficients whose absolute values did not exceed 0.50.

Comparison of Correlation Coefficients of the Mangum and Creta Deposits

Table 12 contains a listing of the correlation coefficients which are 95 percent significantly different between the Creta and Mangum deposits, taking each deposit as a whole.

Several of these correlation coefficients have no

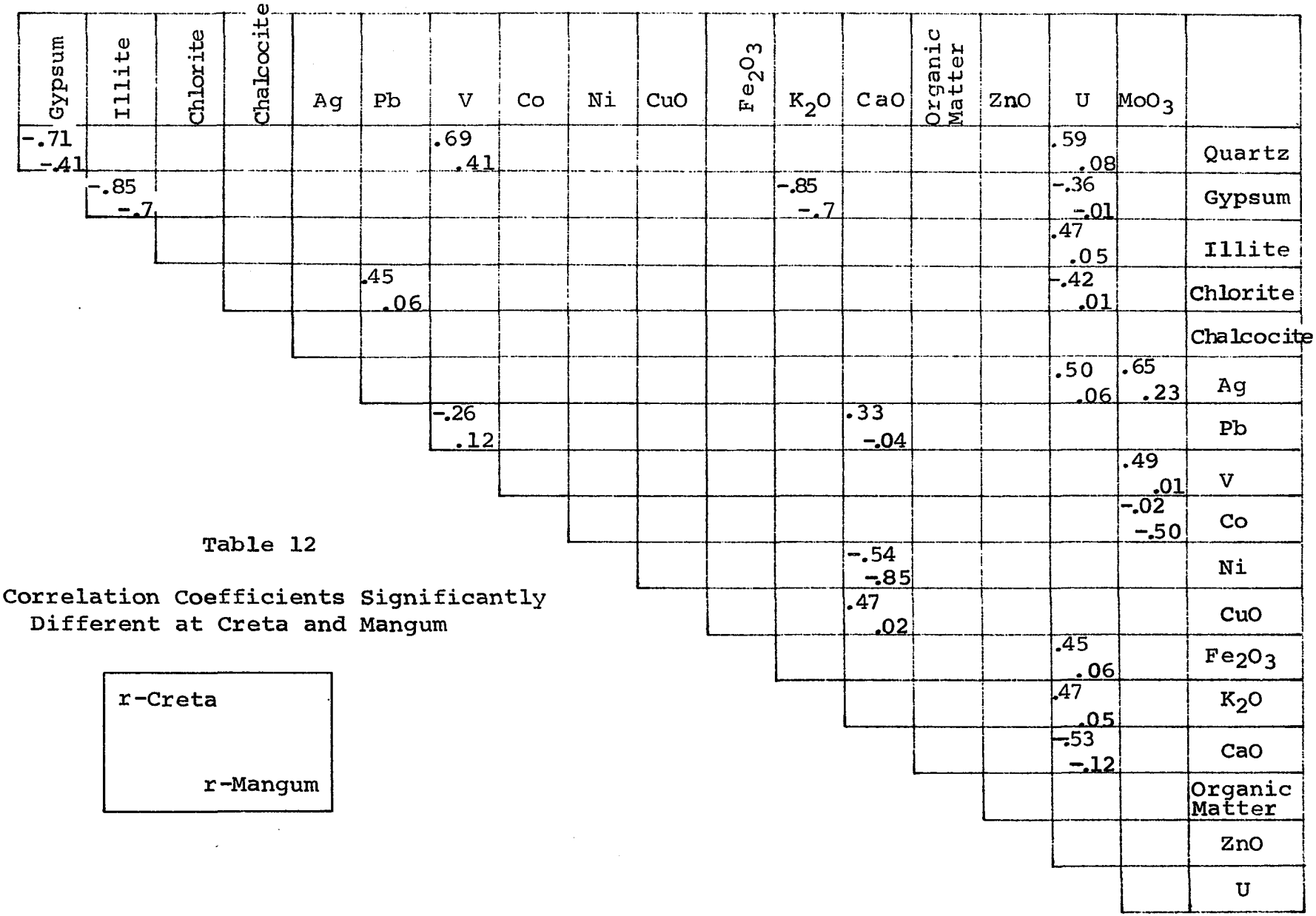

Table 12

Correlation Coefficients Significantly Different at Creta and Mangum

r-Creta

r-Mangum

information content. For example, the uranium-illite and uranium-K_2O correlation coefficients duplicate each other because weight percent illite is calculated directly from weight percent K_2O.

In the case of the Mangum deposit, the standard deviations of quartz, chlorite, and malachite are relatively small compared to Creta (Table 5). The rocks are composed of illite, gypsum, quartz, chlorite, and malachite; however, because the percentages of quartz, chlorite, and malachite do not vary much, gypsum and illite dilute each other. For this reason, there are two sets of correlation coefficients, one for correlation with K_2O (interpreted to be illite), and another set of opposite sign for correlations with gypsum. The situation is complicated slightly in the case of the Creta deposit by the increased variance of quartz, but this dual classification of correlations between gypsum and illite is still appropriate. Because of this dilution we shall deal with only one set of coefficients. The non-redundant lists of important correlation coefficients are as below, (Table 13).

Table 13

Important Correlation Coefficients
Mangum and Creta

	Mangum		Creta
K_2O-silver	+.55		+.66
K_2O-vanadium	+.89		+.87
K_2O-cobalt	+.60		+.53
K_2O-nickel	+.91		+.90
K_2O-iron	+.80		+.83
K_2O-zinc	+.63		----
K_2O-calcium	-.91		-.84
Uranium-lead	-.84		-.77
		Silver-molybdenum	+.65
		Iron-zinc	+.57
		Quartz-uranium	+.59
		Uranium-copper	-.65
		Uranium-calcium	-.53

A number of interpretations explain the correlation coefficients in the upper part of Table 13. There are 5 or 6 elements (Creta and Mangum, respectively) probably associated with illite in 3 types of positions, in the structure, in interlayer positions on the clay mineral grain, or adsorbed on the clay mineral surface. There are, then, 15 or 18 separate hypotheses for the distribution of these elements.

The most direct method of locating the 5 or 6 elements associated with illite is to analyze illite flakes, exchange the adsorbed ions for hydrogen ions, and then re-

analyze the clay mineral flakes. Table 14 presents the results of this part of the research; each specimen having 5 illite clay grains from each sample was analyzed in the JEOL-Princeton Gamma Tech scanning electron microscope-nondispersive analyzer combination. Each grain was counted for three minutes.

Because the properties of illite which could cause adsorption of these elements are common to chlorite, the 5 or 6 elements should be correlated positively to chlorite if adsorption is effective. Because there is no consistent pattern of trace element desorption in either deposit (Table 14), the hypothesis that iron, cobalt, nickel, vanadium, silver, and zinc (Mangum deposit only) are correlated to potassium and illite because of adsorption is rejected (Tables 8, 11). It is not certain whether or not these elements are in interlayer cation positions or structural positions, although from considerations of their electro-negativities and bond lengths, either may be a possibility for some.

The correlation coefficients which are significantly different (95 percent) for Mangum and Creta may be divided into two groups with some internal consistency and a third group of residuals. The first group includes correlations

Table 14 Test of Metal Adsorption on Mangum and Creta Shales

Creta Specimens:	K/Si+K	V/Si+K	Fe/Si+K	Co/Si+K	Ni/Si+K	Ag/Si+K
CN-100 (54.75-60.75)						
before	0.132	0.039	0.219	0.029	0.025	0.011
after	0.272	0.041	0.187	0.031	0.028	0.011
CSP-1 (56.00-62.00)						
before	0.249	0.045	0.132	0.036	0.037	0.014
after	0.295	0.054	0.254	0.042	0.036	0.014
CSP-5 (60.75-76.25)						
before	0.271	0.054	0.252	0.044	0.041	0.018
after	0.154	0.031	0.112	0.022	0.019	0.008
A (0.00-3.00)						
before	0.251	0.056	0.125	0.044	0.040	0.017
after	0.229	0.050	0.223	0.037	0.034	0.016
D (3.00-6.00)						
before	0.230	0.053	0.165	0.042	0.038	0.017
after	0.223	0.038	0.112	0.026	0.022	0.011

Numbers represent ratios of counts from illite flakes, made on the Princeton Gamma Tech-JEOL nondispersive analyzer, and include analyses made before and after ion exchange.

Table 14 (continued)

Mangum Specimens:	K/Si+K	V/Si+K	Fe/Si+K	Co/Si+K	Ni/Si+K	Ag/Si+K	Zn/Si+K
MA (41.25-52.25)							
before	0.225	0.075	0.208	0.052	0.049	0.022	0.043
after	0.322	0.066	0.330	0.052	0.044	0.019	0.037
MC (46.25-49.25)							
before	0.212	0.085	0.216	0.077	0.068	0.033	0.053
after	0.190	0.042	0.140	0.029	0.025	0.012	0.020
ME (62.75-65.75)							
before	0.227	0.036	0.133	0.027	0.023	0.011	0.019
after	0.144	0.027	0.106	0.018	0.016	0.007	0.013
MI (12.25-17.25)							
before	0.251	0.064	0.351	0.051	0.042	0.020	0.038
after	0.186	0.038	0.149	0.025	0.024	0.010	0.019
MG (52.00-55.00)							
before	0.196	0.032	0.120	0.022	0.020	0.009	0.016
after	0.210	0.040	0.177	0.027	0.027	0.011	0.022

Numbers represent ratios of counts from illite flakes, made on the Princeton Gamma Tech-JEOL nondispersive analyzer, and include analyses made before and after ion exchange.

of the following pairs of variables: gypsum-illite, gypsum-potassium, gypsum-quartz, uranium-quartz, uranium-gypsum, uranium-illite, uranium-chlorite, and vanadium-quartz (Table 12). The important feature in the explanation of these correlation coefficients is the higher standard deviations of quartz and gypsum in the Creta deposit (Table 5). The second group includes uranium with illite, chlorite, silver, iron, potassium, and calcium (Table 12).

With the exception of uranium-calcium and uranium-chlorite, the correlations are more positive (or less negative) for Creta. The uranium-calcium correlation appears to be due to increased concentration of calcium in the specimens from the Mangum deposit. The differences between the uranium-chlorite correlations may be due to dilution as a result of increased quartz variance.

The mean concentrations and standard deviations of silver, vanadium, cobalt, iron, and potassium appear to be essentially equal in both deposits (with the possible exception of silver); the difference between the deposits is mainly the oxidation state of some of the sulfur. The comparatively oxidized state of the Mangum deposit and the known propensity of uranium for concentrating in oxidizing media are considered to be responsible for the coefficients

of uranium correlation with silver, iron, and potassium.

Most of the remaining group of correlations which are significantly different (95 percent) between Mangum and Creta are low and may not be real.

Sulfur Isotope Data

A few general principles and findings should be considered before discussing conclusions derived from the sulfur-isotope analyses of the specimens from Creta. Modern sulfate-reducing bacteria can live in significant numbers where the characteristics of the chemical environment vary widely (Baas Becking and others, 1960) and the burial depth is moderate (Feely and Kulp, 1957). Some type of sulfate-reducing bacteria probably have been present throughout much of the history of the earth, particularly in view of the postulated exceedingly early evolution of anaerobes (Cloud, 1971).

It has been observed that there is little difference between the $\delta\ ^{34}S/^{32}S$ of a sulfate solution and the $\delta\ ^{34}S/^{32}S$ of a sulfate mineral, such as gypsum or anhydrite, precipitated from that solution (Holser and Kaplan, 1966).

Nakai and Jensen (1964) have shown that the equi-

librium constant for interchange of ^{34}sulfur and ^{32}sulfur between sulfate ion and sulfide ion is strongly temperature dependent (Fig. 6). As a result the sulfur-isotope ratios of high temperature sulfide deposits converge, and the spread of $\delta\ ^{34}S/^{32}S$ values is relatively small. Conversely, for low temperature deposits, any initial difference of $\delta\ ^{34}S/^{32}S$ will be preserved (Nakai and Jensen, 1964).

Modern experiments on cultures of Desulfovibrio desulfuricans indicate that the isotopic composition of sulfur in bacteriogenic sulfide ion is always much lower than that of the original sulfate ions. Furthermore, these experiments also indicate that when the sulfur-isotope ratio of the dissolved sulfate is constant, the sulfur-isotope ratio of the sulfide ion varies with the rate of sulfide production (Jensen and Nakai, 1964).

Based on the history of sulfur isotopes in sea water (Fig. 7) as constructed by Holser and Kaplan (1966), and the fractionation of approximately 1 part per mil between aquaeous sulfate ion and gypsum, we should expect that the northern and southern gypsum specimens, about 230 million years old, would both have $\delta\ ^{34}S/^{32}S$ values of about +11. The two specimens have $\delta\ ^{34}S/^{32}S$ values of +6.25 and and +4.67, respectively. The narrow range of $\delta\ ^{34}S/^{32}S$ is

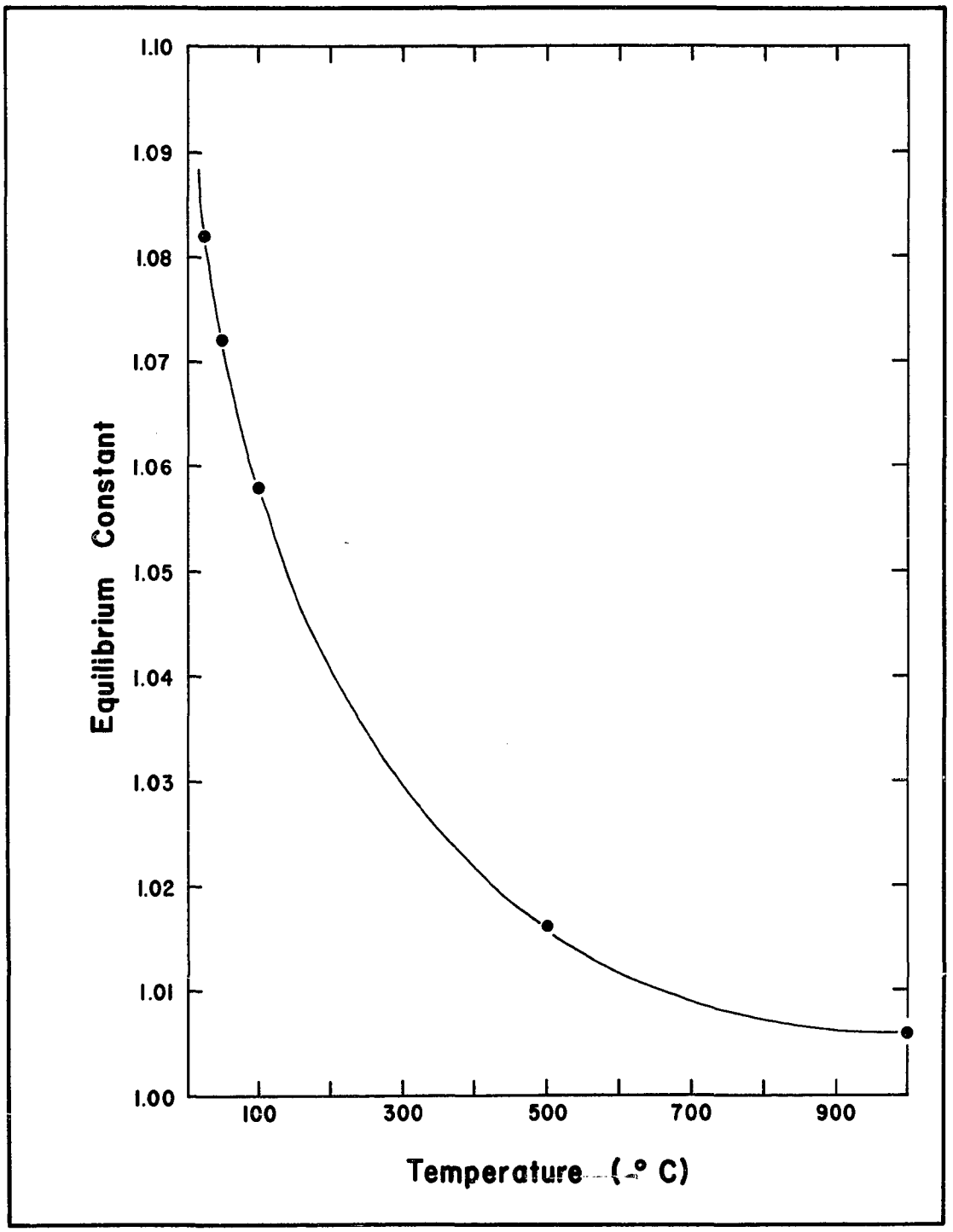

Fig. 6. Approximate fit of experimental data from Nakai and Jensen, (1964), illustrating temperature dependance of equilibrium constant for exchange of sulfur isotopes between sulfate and sulfide ions.

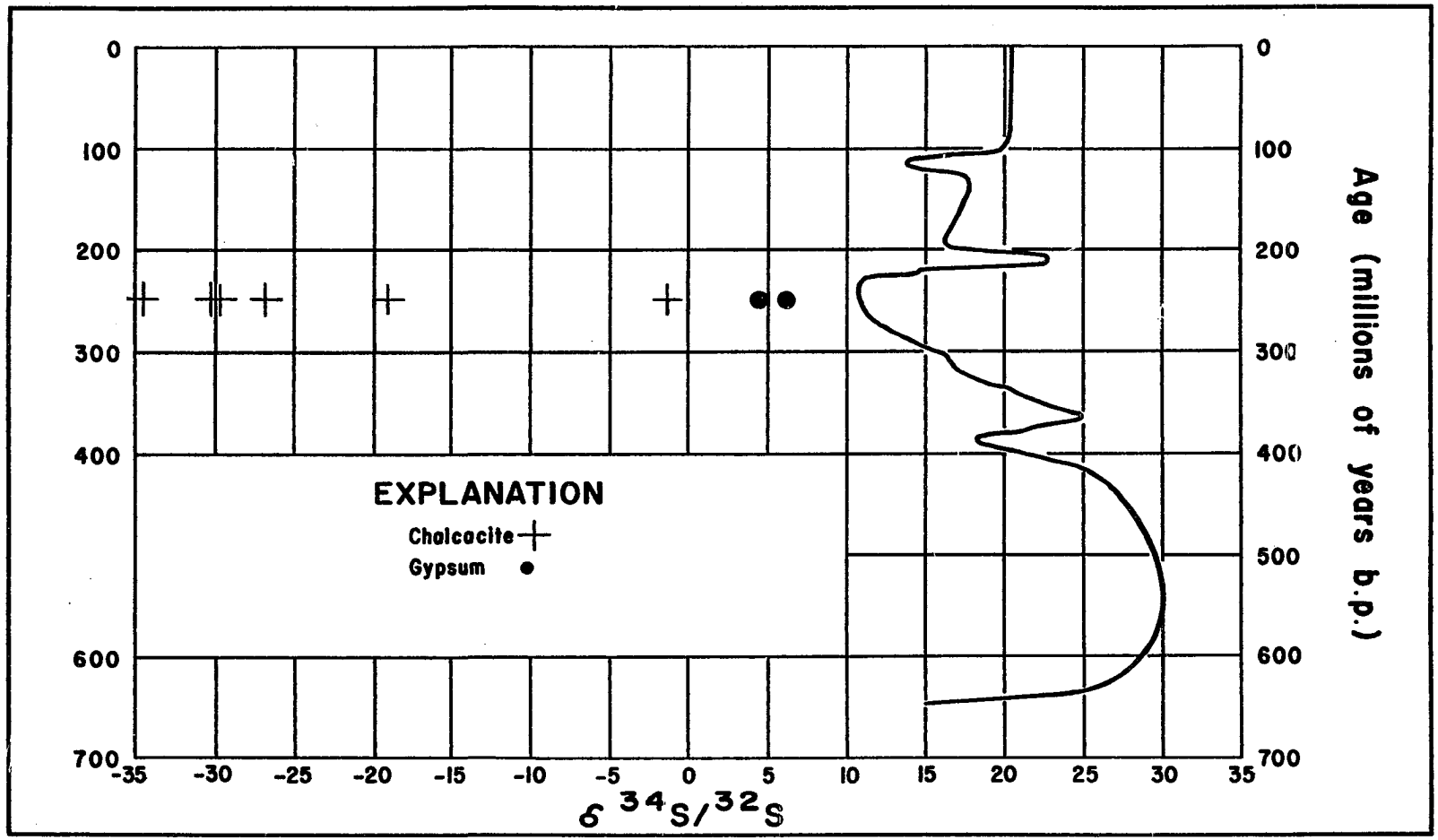

Fig. 7. Relationship between sulfur isotope history of sea water, represented by curve, (Holser and Kaplan, 1966), and Creta gypsums, from the bottom of the gypsum, and chalcocites, from the laminated ore bed below the gypsum. Discussed further in the text.

expected although the sulfur is several parts per mil lighter than expected.

The range of $\delta\ ^{34}S/^{32}S$ for chalcocite concentrates from Creta is from -0.86 to -34.59 parts per mil (Table 4). All of the sulfur-isotope ratios of sulfide are lower than those of sulfate; this is consistent with formation of the sulfide by bacterial reduction of sulfate. Moreover, this range is large compared to the $\delta\ ^{34}S/^{32}S$ range of hydrothermal deposits.

In view of the absence of any correlation between copper content of the Creta and Mangum specimens and any other variable, the interpretation of these sulfur isotope ratios is that the copper minerals present in the unweathered Prewitt copper shale at Creta were originally localized due to reaction with sulfide ion produced by the bacterial reduction of sea water sulfate ion. This localization could have been either syngenetic or diagenetic. The diagenetic hypothesis suggests that the copper minerals may have replaced iron sulfide minerals which had already been precipitated. Cubiform crystals in the Prewitt bed that might be chalcocite pseudomorphs after pyrite are rare, and only a few occurrences have been noted (K. S. Johnson, 1972, oral communication). The only crystal

forms which were recognizable were hexagonal shapes of poor quality, considered to be the forms found on pseudo-hexagonal, orthorhombic chalcocite.

The vertical sections of samples at Creta show only the most diffuse trace of Schurmann-Series zoning, such as has been found in the Kupferschiefer (Wedepohl, 1964). There is no segregation of lead and zinc in succeeding zones of shale above the copper. There are sample sections which have a maximum concentration of silver below the maximum concentration of copper, but this relationship is not consistent throughout the deposit. Because of the apparent lack of zoning, the syngenetic hypothesis, as strictly interpreted, is rejected in favor of the diagenetic origin of chalcocite.

If chalcocite was precipitated either syngenetically or diagenetically, then a minimum activity of bisulfide ion must have obtained. Only with a pH greater than 7 (at 25° C and one atmosphere pressure) will the proper form of sulfur (bisulfide ion) be present. Based on the sulfur-isotope evidence for a sedimentary origin of the chalcocite, the temperature and pressure will be assumed to be 25° C and one atmosphere. Figure 8 shows no chalcocite will be precipitated under these conditions because the fields in

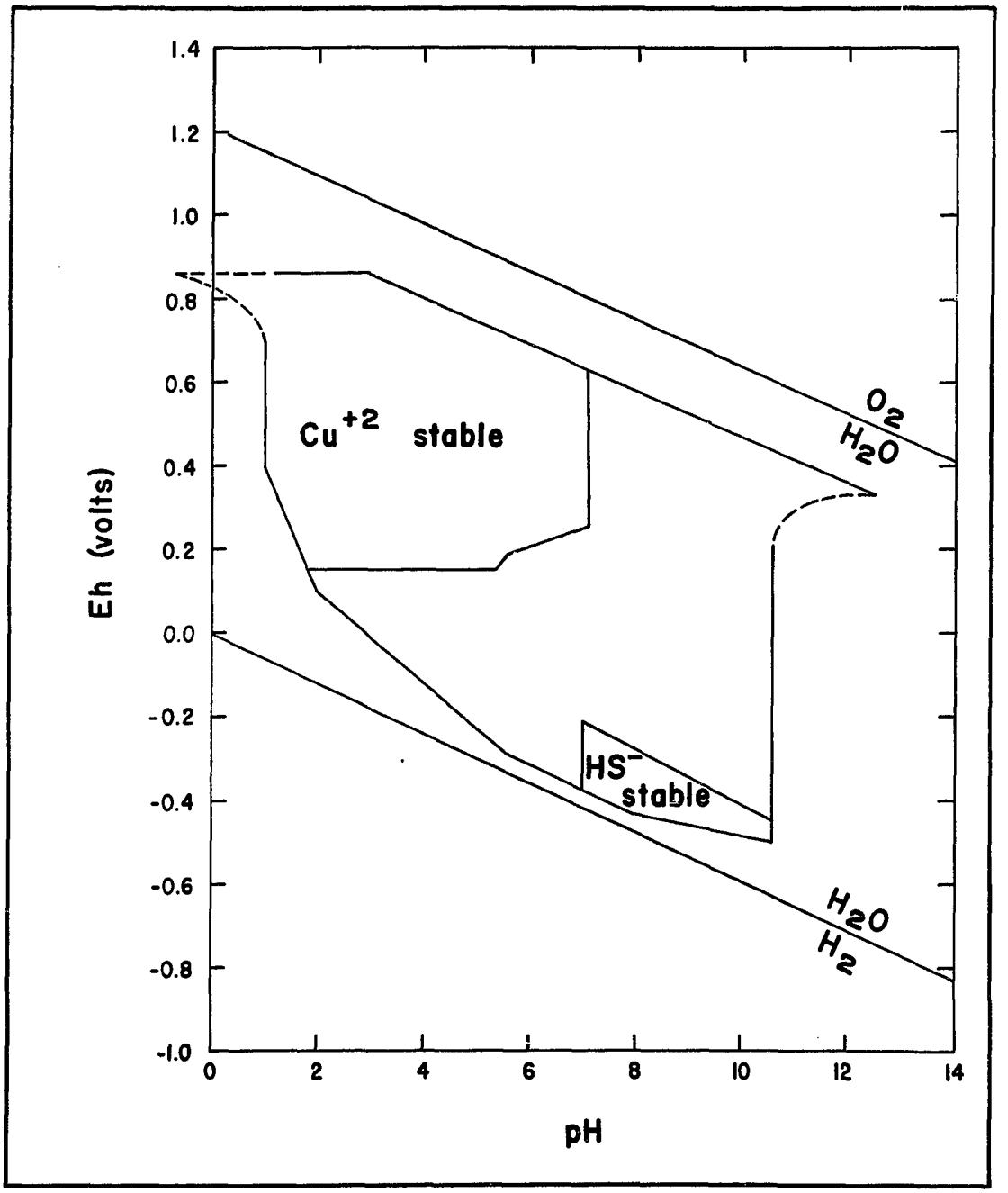

Fig. 8. Eh-pH plots for copper and sulfur. One atmosphere pressure, 25° Centigrade, all boundaries for activity equal to 10^{-6}. Failure of cupric ion and bisulfide fields to overlap illustrates impossibility of precipitating chalcocite where sulfur activity is zero. All other copper fields are oxides or native copper. Discussed further in the text. (Baas Becking and others, 1960; Garrels and Christ, 1965; and Schmitt, H.H., 1962).

which copper and bisulfide ions are stable do not overlap, and there are no stable copper sulfide minerals. If we assume an activity for total dissolved sulfur species of 10^{-1} (Fig. 9), the fields where chalcocite and bisulfide ion are stable do overlap within the fields containing most of the known Eh-pH measurements on natural waters. As a first approximation, the region of overlap defines the approximate range of chemical conditions in which the chalcocite of the Prewitt copper shale at Creta was deposited. Although the actual activity of total dissolved sulfur species may not have been exactly 10^{-1} at Creta, this is a geologically reasonable value.

Comparison of Creta and Manqum Shales to Other Mudrocks

General Statement

Three different approaches have been used in research concerning the chemistry of shales: (1) an attempt to use transition elements and boron to separate marine and nonmarine muds and shales;(2) studies of the metal content of black and bituminous shales; and(3) the origins and environments of deposition of shales of unusual composition, i.e. the manganese shales of Wales (Mohr, 1959).

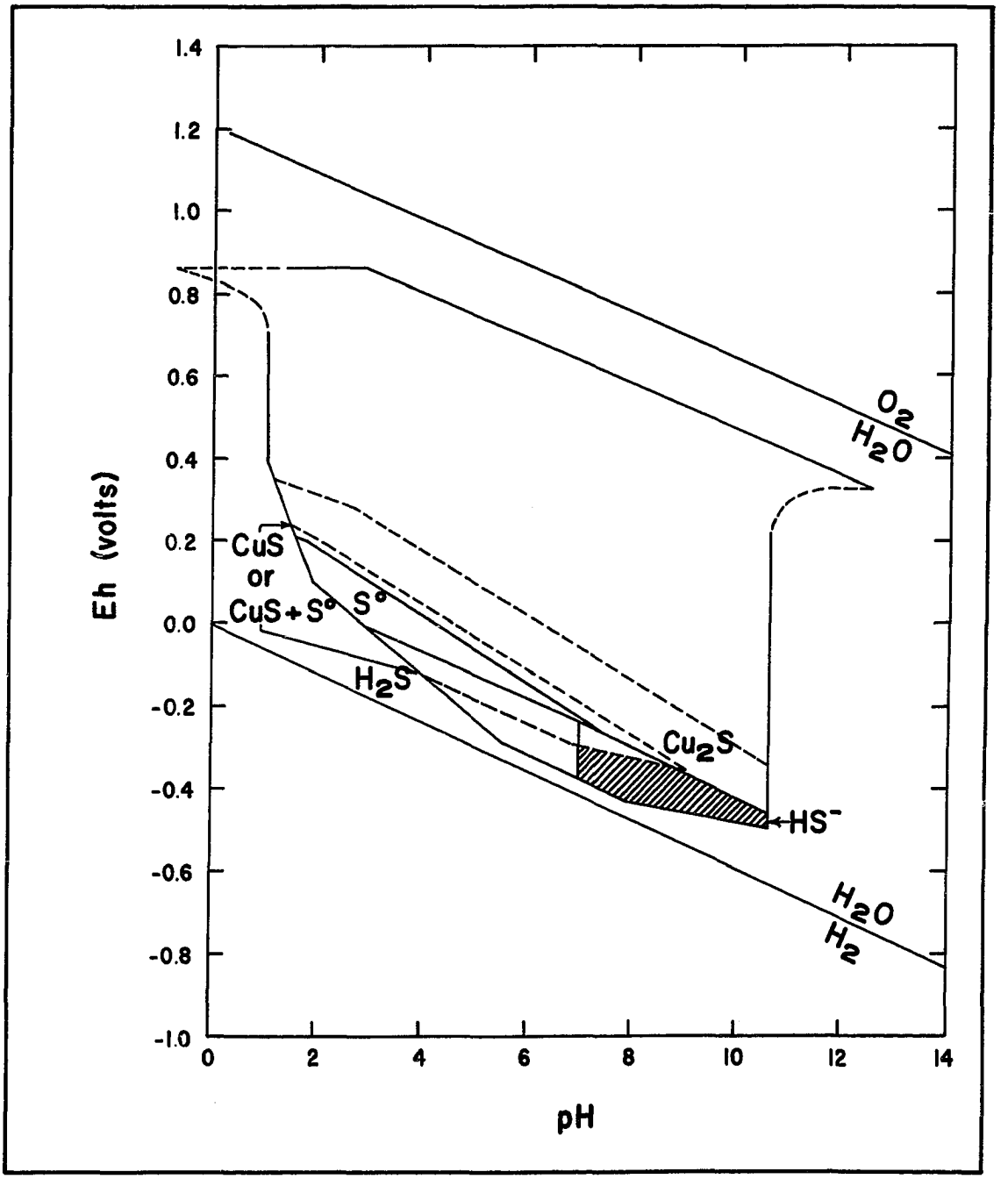

Fig. 9. Eh-pH plots for copper and sulfur, activity of dissolved sulfur equal to 10^{-1}. One atmosphere pressure, 25° Centigrade, all boundaries for activity equal to 10^{-6}. Cross-ruled portion of diagram indicates probable character of diagenetic water which precipitated Creta chalcocites. Discussed further in the text. (Baas Becking and others, 1960; and Schmitt, H. H., 1962).

Trace Metal Content of Marine and Non-marine Shales and Muds

The only useful result of 4 studies of the trace element composition of shales and muds representing a variety of environments of deposition is the observation that marine shales and muds generally have higher boron contents (Degens and others, 1957; Potter and others, 1963; Tourtelot, 1964; and Shimp and others, 1969). However, this cannot be successfully related to illite content, and is therefore of little use in determining paleosalinities.

There are several discrepancies in accounts of the environmental preferences of transition elements. Boron, boron + vanadium, and boron + total clay finer than 2 microns are considered to be the best keys to marine versus non-marine distinctions (Degens and others; 1957; Potter and others, 1963; Tourtelot, 1964), but vanadium alone is considered ineffective (Shimp and others, 1969). Gallium and chromium are found to concentrate in non-marine argillaceous rocks and sediments (Degens and others, 1957; Tourtelot, 1964), or to concentrate marine argillaceous rocks (Potter and others, 1963), or to be distributed more or less equally (Shimp and others, 1969). Nickel has also been found to be concentrated in marine argillaceous

rocks (Degens and others, 1957; Potter and others, 1963) and to be not particularly concentrated in either environment (Shimp and others, 1969). Cobalt, lead, and zinc are not concentrated in either marine or non-marine argillaceous rocks in any of the 4 studies cited.

Shale Types in the Creta Deposit

For a 90 percent level of significance, only the concentrations of illite, gypsum, cobalt, nickel, organic matter, zinc, and calcium are identical in the barren gray shales and the copper-rich gray shales (Table 10). If the copper minerals were deposited by reduction of copper-bearing oxidizing solutions moving through the rocks, the copper-rich shales should be relatively deficient in organic matter due to its consumption in reducing the copper-bearing solutions. The fact that they are not so depleted may indicate that some of the organic matter in these rocks is not inherited from deposition.

For a classification of shales based on 3 colors (red, gray, and maroon), complete testing requires an "accept" or "reject" for a particular variable for each of 3 separate comparisons, gray-red, gray-maroon, and red-maroon. Due to a single hypothesis which did not satisfy the assumption for one color pair, we must assume that a

common decision in the other 2 hypotheses for that variable fixes the untestable hypothesis's decision to a level of significance near that of the 2 tests. Accordingly, the concentrations of quartz, uranium, and organic matter are equal in red, gray, and maroon shales; and the concentrations or iron, nickel, and chlorite are unequal in the 3 groups of shales. The concentrations of illite, vanadium, potassium, calcium, and zinc are equal in red and gray shales, for a significance level of 90 percent (Table 10).

Shale Types in the Mangum Deposit

The shales in the Mangum deposit were divided into 5 classes: gray, mottled, red, maroon, and shales with more copper than the average for the deposit. The concentrations of quartz, gypsum, illite, chlorite, vanadium, cobalt, and potassium are identical for the classes based on color. The only significant differences between silver and iron contents of shales is between red and gray shales; for nickel, the only significant differences (95 percent level) are between gray and mottled shales, and between gray and red shales (Table 7).

Copper-Rich and Common Gray Shales at Creta

The differences between common gray and copper-rich

gray shales for the Creta deposit are as follows: higher quartz, silver, vanadium, iron, potassium, uranium, and molybdenum concentrations in the gray shales; and significantly higher concentrations of chlorite, lead, and copper in the copper-rich shales (Table 10). Silver, vanadium, and iron are more abundant in the gray shales (Table 8) probably because of the higher content of illite.

Copper-Rich and Common Gray Shales at Mangum

The differences between the gray and copper-rich shales in the Mangum deposit are as follows: concentrations of uranium and molybdenum are higher in the gray shales, whereas malachite, lead, cobalt, and copper are relatively concentrated in the copper-rich shales (Table 7). The higher concentration of malachite and copper in the shales which were classed by their greater-than-average copper content is understandable. However, the difference between the molybdenum and uranium contents of copper-rich and gray shales is not explainable on the basis of the data. There are only two significant correlation coefficients (uranium-lead, uranium-cobalt) for uranium in either copper-rich or gray shales (uranium-lead and uranium-cobalt); in each case the value and sign of the coefficients are signi-

ficantly equal (Table 11). Moreover, there are no significant correlations of molybdenum with any other variable in gray copper-rich shale. Lead correlates significantly only to cobalt in gray and copper-rich shales, and the difference between the lead-cobalt coefficients for the two types of shale is insignificant. The data do not suggest a model for the mode of occurrence of lead in either type of shale.

CONCLUSIONS

Because there is no indisputable evidence of unique concentrations of most of the analyzed variables, and because of uncertainty regarding concentrations of several elements on marine and non-marine clays, we cannot assign a generalized paleosalinity to either the Prewitt or Meadows copper shales. The work of Wilson (1962) and Clapham (1970) suggests a brackish or marine environment during deposition of gray shales in the formation. In addition, we may infer hypersalinity at Creta during deposition of the Prewitt copper shale, as evidenced by the gypsum bed immediately overlying the ore.

The large grains of gypsum in the samples from both Creta and Mangum are far out of hydraulic equivalence with the accompanying small clay and quartz particles: this is taken as evidence that gypsum precipitated diagenetically in the mud.

The range of $\delta\,^{34}S/^{32}S$ values of chalcocite concentrates from Creta and the maximum value being lower

than the normal marine gypsum lead me to conclude that the chalcocite is syngenetic or diagenetic. Moreover, the absence of Schurmann's Series of metal enrichment above the Prewitt copper shale, as is found in the Kupferschiefer, leads me to conclude that the chalcocite is diagenetic.

The shales in the Creta and Mangum deposits are "normal" in many respects; indeed, only copper and lead are in abnormally high concentrations in the copper-rich shales. No geochemical criteria for assigning specific environments of deposition to any of the shales sampled in either of the deposits were discovered.

The copper shales in the Mangum deposit have the same general pattern of compositional relationships as do the shales in the Creta deposit. This is true also of the non-cupriferous shales in each deposit. This observation and the observation that the copper shale at Creta contains malachite instead of chalcocite when the overburden is less than 10 to 20 feet suggest that the Meadows copper shale at Mangum was oxidized by meteoric waters, and is the analog of the Prewitt copper shale at Creta.

REFERENCES CITED

Baas Becking, L. G. M., Kaplan, I. R., and Moore, D., 1960, Limits of the Natural Environment in Terms of pH and Oxidation-Reduction Potentials: Jour. Geol., vol. 68, p. 243-284.

Brongersma-Sanders, M., 1968, On the Geographical Association of Strata-Bound Ore Deposits with Evaporites: Mineral. Deposita, vol. 3, p. 286-291.

Brown, A. C. and Trammell, J. W., 1966, Zoning of the White Pine Copper Deposit, Ontonagon Co., Michigan: Econ. Geol., vol. 61, p. 1308.

Cameron, E. N., 1964.

Clapham, W. B., Jr., 1970, Nature and Paleogeography of Middle Permian Floras of Oklahoma as Inferred from their Pollen Record: Jour. Geol., vol. 78, p. 153-171.

Cloud, P. C., 1971, A Working Model of the Primitive Earth (abs.): Abstracts with Programs, Geol. Soc. America, vol. 3, 800 p.

Cuthbert, M. E., 1962, Formation of Bornite at Atmospheric Temperature and Pressure: Econ. Geol., vol. 57, p. 38-41.

Davidson, C. F., 1964, Uranium in Ancient Conglomerates: A Review: Econ. Geol., vol. 59, p. 168-177.

_____, 1965, A Possible Mode of Origin of Strata-Bound Copper Ore: Econ. Geol., vol. 60, p. 942-954.

Davidson, D. F. and Lakin, H. W., 1961, Metal Content of Some Black Shales of the Western United States: U. S. Geol. Surv. Prof. Pap. 424-C, Article 267, p. C329-C331.

Deans, T., 1950, The Kupferschiefer and the Associated Lead-Zinc Mineralization in the Permian of Silesia, Germany, and England: Part VII, Eighteenth Session of the International Geological Congress, London, p. 340-351.

Deer, W. A., Howie, R. A., and Zussman, J., 1962, Rock-forming Minerals, vol. 3, Sheet Silicates: New York, John Wiley and Sons, Inc., 270 p.

Degens, E. T., Williams, E. G., and Keith, M. L., 1957, Environmental Studies of Carboniferous Sediments Part 1: Geochemical Criteria for Differentiating Marine from Fresh-Water Shales: Bull. of the Amer. Assoc. Petrol. Geol., vol. 41, p. 2427-2455.

Dunham, K. C., 1962, Neptunist Concepts in Ore Genesis: Econ. Geol., vol. 59, p. 1-21.

Feely, H. W. and Kulp, J. L., 1957, Origin of Gulf Coast Salt-Dome Sulfur Deposits: Bull. Amer. Assoc. Petrol. Geol., vol. 41, 1802-1853.

Fischer, R. P., 1937, Sedimentary Deposits of Copper, Vanadium-Uranium, and Silver in Southwestern United States: Econ. Geol., vol. 32, p. 906-951.

Flanagan, F. J., U. S. Geological Survey Standards--II. First Compilation of Data for the New U. S. G. S. Rocks: Geochim. et Cosmochim. Acta, vol. 33, p. 81-120.

Garlick, W. G., 1963, Hydrothermal Versus Syngenetic Theories of Ore Deposition: Econ. Geol., vol. 58, p. 447-456.

_____, 1964, Association of Mineralization and Algal Reef Structures on Northern Rhodesian Copperbelt: Econ. Geol., vol. 59, p. 416-427.

Garrels, R. M. and Christ, C. L., 1965, Solutions, Minerals, and Equilibria: New York, Harper and Row, 450 p.

Gaucher, E., 1964, A Possible Solution to the Paradox of the "Sedimentary" Bornite: Econ. Geol., vol. 59, p. 303-308.

General Electric, 1965, X-ray Periodic Chart: Milwaukee, General Electric Co.

Ham, W. E. and Johnson, K. S., 1964, Copper Deposits in the Permian Shale, Creta Area: Okla. Geol. Surv. Circular 64, 32 p.

Ham, W. E., Denison, R. E., and Merritt, C. A., 1964, Basement Rocks and Structural Evolution Southern Oklahoma: Okla. Geol. Surv. Bull. 95, 302 p.

Holser, W. T. and Kaplan, I. R., 1966, Isotope Geochemistry of Sedimentary Sulfates: Chem. Geol., vol. 1, p. 93-135.

Jackson, M. L., 1958, Soil Chemical Analysis: Englewood Cliffs, New Jersey, Prentice-Hall, Inc. 498 p.

Jensen, M. L. and Nakai, N., 1964, Large Scale Bacteriogenic Fractionation of Sulphur Isotopes: Pure and Applied Chemistry, vol. 8, p. 305-315.

Johnson, K. S., 1965.

_____, 1971.

_____, 1972.

Kalliokoski, J., 1966, Diagenetic Pyritization in Three Sedimentary Rocks: Econ. Geol., vol. 61, p. 872-885.

Kaye, M. J., 1965, X-ray Fluorescent Determinations of Several Trace Elements in Some Standard Geochemical Samples: Geochim. et Cosmochim. Acta, vol. 29, p. 139-143.

Krauskopf, K. B., 1955, Sedimentary Deposits of Rare Metals: Econ. Geol., Fiftieth Anniv. Vol., p. 411-463.

Ljunggren, P. and Meyer, H. C., 1964, The Copper Mineralization in the Corocoro Basin, Bolivia: Econ. Geol., vol. 59, p. 110-125.

Love, J. D., 1961, Vanadium and Associated Elements in the Phosphoria Formation in the Afton Area, Wyoming: U. S. Geol. Surv. Prof. Pap. 424-C, Article 250, p. C279-C282.

Love, L. G., 1962, Biogenic Primary Sulfide of the Permian Kupferschiefer and Marl Slate: Econ. Geol., vol. 57, p. 350-366.

Malan, S. P., 1964, Stromatolites and Other Algal Structures at Mufulira, Northern Rhodesia: Econ. Geol., vol. 59, p. 397-415.

McCauley, J. F., 1958, Supergene Copper-Uranium Deposits, Nova Scotia: Econ. Geol., vol. 53, p. 1038-1042.

Miser, H. D. and others, Geologic Map of Oklahoma: Okla. Geol. Surv. Map., 1:500,000.

Mohr, P. A., 1959, A Geochemical Study of the Shales in the Lower Cambrian Manganese Shales Group of the Harlech Dome, North Wales: Geochim. et Cosmochim. Acta, vol. 17, p. 186-200.

Nakai, N. and Jensen, M. L., 1964, The Kinetic Isotope Effect in the Bacterial Reduction and Oxidation of Sulfur: Geochim. et Cosmochim. Acta, vol. 28, p. 1893-1912.

Nishihara, H., 1957, Origin of the "Manto" Copper Deposits in Lower California, Mexico: Econ. Geol., vol. 52, p. 944-951.

Noble, E. A., 1963, Formation of Ore Deposits by Waters of Compaction: Econ. Geol., vol. 58, p. 1145-1156.

Ostle, B., 1963, Statistics in Research: Second Edition, Ames, Iowa, Iowa State Univ. Press, 585 p.

Paltridge, I. M., 1968, An Algal Biostrome Fringe and Associated Mineralization at Mufulira, Zambia: Econ. Geol., vol. 63, p. 207-217.

Park, C. F., Jr. and MacDiarmid, R. A., 1964, Ore Deposits: San Francisco, W. H. Freeman and Co., 475 p.

Poole, A. B., 1968, A Second Report on the Standard Rocks QMC I1, QMC I3, QMC M2, and QMC M3.

Potter, P. E., Shimp, N. F., and Witters, J., 1963, Trace Elements in Marine and Fresh-Water Argillaceous Sediments: Geochim. et Cosmochim. Acta, vol. 27, p. 669-694.

Richardson, P. W. and Hawkes, H. E., 1958, Adsorption of Copper on Quartz: Geochim. et Cosmochim. Acta, vol. 15, p. 6-9.

Roberts, W. M. B., 1963, The Low Temperature Synthesis in Aquaeous Solution of Chalcopyrite and Bornite: Econ. Geol., vol. 58, p. 52-61.

Roubalt, M., de la Roche, H. and Govindaraju, K., 1966, Report on Four Geochemical Rock Standards: Granites GR, GA, GH, and Basalt BR: Centre de Recherches Petrographiques et Geochimiques, C. N. R. S., Nancy.

Schmitt, H. H., (Editor), 1962, Equilibrium Diagrams for Minerals at Low Temperature and Pressure: Cambridge, Mass., Geol. Club of Harvard, 199 p.

Serkies, J., Krason, J., and Idzikowski, A., 1965, On Some Differences between Formation Processes in the North-Sudetic Copper Deposits as Results of Supergenic Changes: Bull. de L'Acad. Polonaise des Sci., Ser. des sci. geol. et geogr., vol. 13, p. 195-200.

Shimp, N. F., Witters, J., Potter, P. E., and Schleicher, J. A., 1969, Distinguishing Marine and Freshwater Muds: Jour. Geol., vol. 77, p. 566-580.

Slowey, J. F. and Jeffrey, L. M., 1967, Evidence for Organic Complexed Copper in Sea Water: Nature, vol. 214, p. 377-378.

Solomon, P. J., 1965, Investigations into Sulfide Mineralization at Mount Isa, Queensland: Econ. Geol., vol. 60, p. 737-765.

Soule, J. H., 1956, Reconnaissance of the "Red Bed" Copper Deposits in Southeastern Colorado and New Mexico: U. S. Bur. Mines Inf. Circ. 7740, 74 p.

Stroud, R. B., McMahan, A. B., Stroup, R. K., and Hibpshman, M. H., 1970, Production Potential of Copper Deposits Associated with Permian Red Bed Formations in Texas, Oklahoma, and Kansas: U. S. Bur. Mines Rep. of Investigations 7422, 103 p.

Temple, K. L. and LeRoux, N. W., 1964, Syngenesis of Sulfide Ores: Desorption of Adsorbed Metal Ions and Their Precipitation as Sulfides: Econ. Geol., vol. 59, p. 647-655.

Thomas, W. K. L. and Kempe, D. R. C., 1963, Standard Geochemical Sample T-1, Msusule Tonalite, Supplement No. 1: Dar es Salaam, Geol. Surv. Div., Ministry of Commerce and Industry, 6 p.

Tourtelot, H. A., 1964, Minor-Element Composition and Organic Carbon Content of Marine and Nonmarine Shales of Late Cretaceous Age in the Western Interior of the United States: Geochim. et Cosmochim. Acta, vol. 28, p. 1579-1604.

Trask, P. D., 1925, The Origin of the Ore of the Mansfeld Kupferschiefer, Germany, A Review of the Current Literature: Econ. Geol., vol. 20, p. 746-761.

Vine, J. D., 1966, Element Distribution in Some Shelf and Eugeosynclinal Black Shales: U. S. Geol. Surv. Bull. 1214-E, 31 p.

_____, 1969, Element Distribution in Some Paleozoic Black Shales and Associated Rocks: U. S. Geol. Surv. Bull. 1214-G, 32 p.

Vine, J. D., Tourtelot, E. B., and Keith, J. R., 1969, Element Distribution Some Trough and Platform Types of Black Shale and Associated Rocks: U. S. Geol. Surv. Bull. 1214-H, 38 p.

Ward, P. E., 1963, Shallow Halite in Flowerpot Shale of Southwestern Oklahoma: U. S. Geol. Surv. Prof. Pap. 450-E, Article 190, p. E40-E42.

Wedepohl, K. H., 1964, "Kupferschiefer" and the Problem of Syngenetic Ore Deposition: (abs.), Geol. Soc. America Bull., vol. 75, p. P187.

White, W. S., 1960, The White Pine Copper Deposit: Econ. Geol., vol. 55, p. 402-409.

White, W. S. and Wright, J. C., 1954, The White Pine Copper Deposit, Ontonagon County, Michigan: Econ. Geol., vol. 49, p. 675-716.

Wilson, L. R., 1962, Permian Plant Microfossils from the Flowerpot Formation, Greer County, Oklahoma: Okla. Geol. Surv. Circ. 49, 50 p.

APPENDIX I

STRATIGRAPHIC SECTIONS OF THE MANGUM PITS

For locations, see Figure 3

Pit	Interval (inches)	Description
MA	0.00-12.50	Claystone. greenish-gray. Beds to 1.5 inches thick. clay 95%, sand and black material on joints 2%. Structure: blocky.
	12.50-17.00	Claystone. maroon. Texture: blocky, beds to 1.5 inches thick. Mineralogy: clay 95%, traces of black material on joints.Small (3/4 mm.) diameter rounded white beads of gypsum on weathered surface.
	17.00-20.00	Shale. Color: reddish-maroon. Texture: sometimes fissile. Mineralogy: clay 95%.
	20.00-25.00	Shale. Color: mottled maroon and green. Texture: fissile.
	25.00-32.00	Sandy shale. Color: buff-orange. Texture: bimodal, approximately 30% sand. Mineralogy: gypsum 30%, clay 60%, limonite (?) 10%.

APPENDIX I (continued)

Pit	Interval (inches)	Description
MA	32.00-41.25	Shale. Color: red, mottled red and gray-green from 34.00 to 41.25. Texture: fissile, very fine-grained. Mineralogy: clay 95%.
	41.25-52.25	Shale. Color: green-gray. Texture: semi-fissile, forms 1/2 inch diameter rounded beads from combination of bedding and jointing. Mineralogy: clay, 95%.
	52.25-66.25	Meadows Copper Shale. Color: gray-green with bright green plates on bedding planes. Texture: fissile, very fine-grained. Mineralogy: clay 55%, malachite 10%, sand-size dolomite (?) 30%. Dolomite (?) mainly at base.
MB	0.00-20.00	Soil, reddish
	20.00-40.50	Shale. Color: green-gray. Texture: very fine-grained, basal 4 inches laminated. upper part of interval blocky when fresh, fissile on weathered surface.
	40.50-41.75	Shale. Color: mottled maroon and light gray. Mottlings only generally parallel bedding. Texture: very fine-grained.

APPENDIX I (continued)

Pit	Interval (inches)	Description
MB	41.75-64.00	Shale. Color: mottled green (80%) and chocolate (20%). Texture: very fine-grained, nonlaminated from 41.75 to 56.00 inches, laminated from 56.00 to 64.00 inches, fissile.
	64.00-71.00	Shale. Color: red. Texture: fissile, very fine-grained, nonlaminated. Mineralogy: very gypsiferous, includes 1/2 inch Gypsum from 1.00 to 1.50 inches from top.
	71.00-72.00	Gypsum.
	72.00-down	Shale. Color: green. Very gypsiferous.
MC	0.00-19.00	Soil.
	19.00-33.00	Shale. Color: red, irregularly mottled green except for green shale mottled red for basal 2 inches. Mottling not stratigraphic. Mineralogy: highly gypsiferous, including 1/2 inch seam of alabaster gypsum from 28.25 to 28.75 inches. Also some dispersed dolomite (?) or gypsum sand.

APPENDIX I (continued)

Pit	Interval (inches)	Description
MC	33.00-38.50	Gypsum. Upper 3 inches is alabaster. Lower thickness is alternating satinspar layers (prisms vertical) and clay layers, which are mainly washed out. Maximum thickness of satinspar layer is 3/8 ths inch, clay layers usually about 5/8 ths inch thick.
	38.50-44.75	Shale. Color: gray-green, 10% is dark reddish-gray, almost maroon. Distribution unknown--does not appear to be stratabound. Texture: fissile, nonlaminated.
	44.75-46.25	Gypsum. Color: alternating dark gray-green bands and pink-white bands. Structure: laminated, band thickness 1/8 to 3/8 inch.
	46.25-56.00	Shale. Color: gray-green from 46.25 to 49.25, maroon from 49.25 to 53.25, and gray-green from 53.25 to 56.00.
	56.00-66.00	Claystone. Color: gray-green. Texture: very fine-grained except for gypsum crystals up to 1/4 inch diameter. Massive, hard, nonlaminated. Mineralogy: clay 70%, quartz, gypsum 25%.

APPENDIX I (continued)

Pit	Interval (inches)	Description
MC	66.00-67.00	Claystone. Color: red-brown. Texture: massive, except for gypsum, very fine grained. Mineralogy: 20-30% gypsum, clay and quartz 70-80%.
	67.00-68.00	Claystone. Color: gray-green. Otherwise same as from 56.00-66.00.
	68.00-77.50	Gypsiferous shale. Color: red-brown mainly but with about 15% green in 2 blotches, one rounded one and one green shale layer at 76.50 to 77.50 inches.
MD	0.00-11.00	Soil. Structure: obscure. Primarily grayish-pink.
	11.00-12.50	Shale. Color: maroon.
	12.50-14.50	Shale. Color: mottled, gray-green with bedding streaks of maroon.
	14.50-23.75	Shale. Color: mottled, mainly red with non-strata-bound light gray-green blotches.
	23.75-35.25	Shale. Color: medium gray. Texture: very fine-grained, fissile, nonlaminated, beady. Mineralogy: clay, quartz.

APPENDIX I (continued)

Pit	Interval (inches)	Description
MD	35.25-48.25	Meadows Copper Shale. Color: gray with green plates and stains on fissility planes and on curved joint planes on beads. Texture: very fine-grained. Mineralogy: clays and quartz 90%, malachite 10%,, included in interval are a bed of Gypsum from 42.63 to 42.88 inches, and buff dolarenite from 47.75 to 48.25 inches.
	48.25-59.50	Shale. Color: gray.
ME	0.00-4.63	Soil, primarily loose rubble of Dolomite.
	4.63-7.50	Marty Dolomite. Badly weathered, semi-coherent. Color: light gray. Texture: fine-grained, beds about 1/2 inch thick.
	7.50-11.75	Shale. Badly weathered. Color: gray. Texture: very fine-grained, fissile.
	11.75-18.75	Shale. Badly weathered. Color: mottled, mainly red with minor gray, mottling not parallel bedding. Texture: very fine-grained, fissile.
	18.75-21.25	Shale. Color: gray. Texture: very fine-grained.
	21.25-26.00	Shale. Color: maroon. Texture: fissile, very fine-grained.

APPENDIX I (continued)

Pit	Interval (inches)	Description
ME	26.00-28.50	Shale. Color: gray. Texture: very fine-grained.
	28.50-31.13	Dolarenite layer.
	31.13-37.25	Shale. Color: gray. Texture: very fine-grained.
	37.25-40.38	Argillaceous sandstone. Color: light gray-green. Texture: laminated. Mineralogy: clay 30%, quartz 70%.
	40.38-41.88	Shale. Color: gray. Texture: very fine-grained.
	41.88-42.00	Shale. Color: brown.
	42.00-42.75	Dolarenite layer.
	42.75-52.25	Gypsiferous shale. Color: red, includes brown shale from 44.75 to 44.88 inches, and laminated sandy gray shale from 44.88 to 45.25 inches. Texture: fine-grained with additional sand from 42.75 to 45.25 inches, includes crystals of gypsum with diameter of up to 1/4 inch. Fissile.
	52.25-54.75	Shale. Color: gray.
	54.75-55.88	Shale. Color: red.
	55.88-62.75	Shale. Color: gray. Noncupriferous.

APPENDIX I (continued)

Pit	Interval (inches)	Description
ME	62.75-65.75	Meadows Copper Shale. Color: gray with bright green spots and irregular stains on the bedding planes. Texture: very fine-grained, fissile. Mineralogy: clay and fine quartz 90%, malachite 10%.
	65.75-66.38	Dolarenite layer.
	66.38-71.50	Gypsiferous shale. Color: red.
MF	0.00-2.00	Soil.
	2.00-20.00	Gypsum. Color: light greenish-white. Texture: laminated, beds to 3 1/4 inches thick. Mineralogy: gypsum, clay washed out.
	20.00-33.50	Gypsum. Color: from 20.00 to 24.50 inches, gypsum is light green and shale stringers are red. From 24.50 to 33.50 inches, both gypsum and shale are red. Mineralogy: gypsum 85%, shale 15%.
	33.50-36.00	Shale. Color: red, one 1/2 inch thick green bed. Texture: fissile, soft.
	36.00-53.13	Shale. Color: gray-green. Texture: fissile, laminated, laminae thickness 1/8 th inch. Mineralogy: clay and quartz.

APPENDIX I (continued)

Pit	Interval (inches)	Description
MF	53.13-61.00	Meadows Copper Shale. Color: gray-green with bright green spots on bedding planes. Texture: very fine-grained. Mineralogy: clay and quartz 90%, malachite 10%. Bottom very irregular. Includes Dolarenite layer from 57.38 to 57.88 inches.
	61.00-down	Shale. Color: red-brown. Texture: very fine-grained except for gypsum crystals up to 1/4 inch length. Mineralogy: clay and quartz 80%, gypsum 20%.
MG	0.00-15.00	Rubble of Gypsum
	15.00-24.50	Gypsum. Color: white. Mineralogy: alabaster.
	24.50-41.50	Gypsiferous shale. Color: red. Texture: very fine-grained matrix of clay, quartz, etc., gypsum crystals up to 1 inch length parallel the bedding, thickness usually 1/8 to 1/16 th inch. Mineralogy: about 50% gypsum.
	41.50-52.00	Shale. Color: gray-green. Texture: very fine-grained, laminated, fissile.

APPENDIX I (continued)

Pit	Interval (inches)	Description
MG	52.00-61.25	Meadows Copper Shale. Color: gray-green with bright green spots in bedding planes. Texture: very fine-grained, has rare gypsum veinlets. Structure: slope of top of copper zone is about 1 inch in 12 inches to the south, relative to bedding. Includes gypsum layer from 58.25 to 58.50 inches, and extra gypsiferous layer from 60.75 to 61.25 inches.
	61.25-67.00	Gypsiferous shale. Color: gray-green. Noncupriferous.
	67.00-down	Shale. Color: red-brown. Mineralogy: very gypsiferous, includes 7/8 ths inch thick gypsum vein dipping 70-80°.
MH	0.00-4.00	Marty Dolomite. Color: tan, weathered surface.
	4.00-9.50	Structureless subsoil. Parent material is gray shale, weathering yellow-gray. Very fine-grained.
	9.50-19.75	Shale. Color: gray, weathering yellow-gray.
	19.75-24.75	Shale. Color: maroon, mottled with gray. Texture: very fine-grained.

APPENDIX I (continued)

Pit	Interval (inches)	Description
MH	24.75-41.25	Shale. Color: gray. Texture: fissile, very fine-grained.
	41.25-47.50	Gypsum. Color: gypsum is pink with interbeds of maroon shale. Interbeds of shale up to 1 inch thick.
	47.50-61.25	Shale. Color: red-brown (no fresh surfaces). Texture: fissile, very fine-grained.
	61.25-77.75	Shale. Color: gray. Texture: fissile, very fine-grained.
	77.75-78.00	Gypsum.
	78.00-78.38	Dolarenite layer.
	78.38-78.88	Shale. Color: gray, green spots on bedding planes. Texture: very fine-grained.
	78.88-81.25	Gypsum. Color: gray-green. Texture: massive, crystal size unknown. Mineralogy: alabaster, includes only a little shale.
	81.25-89.00	Meadows Copper Shale. Color: gray, green spots to 1/2 inch diameter on bedding planes. Texture: very fine-grained, laminated, fissile. Includes several 1/8 th inch thick satinspar beds.

APPENDIX I (continued)

Pit	Interval (inches)	Description
MH	89.00-91.00	Gypsiferous shale. Color: red-brown.
MI	3.50-0.00	Argillaceous sandstone. Color: yellow-green. Mineralogy: quartz 70%, clay 30%.
	+0.00-3.88	Shale. Color: gray-green. Texture: very fine-grained.
	3.88-6.63	Shale. Color: red. Texture: upper and basal inches very fine-grained, middle 3/4 ths inch sandy.
	6.63-12.25	Shale. Color: reddish-gray. Texture: fissile, very fine-grained.
	12.25-26.13	Meadows Copper Shale. Color: gray with green spots on bedding planes, and yellow-orange stains on joint planes. Texture: very fine-grained, fissile. Mineralogy: clay, quartz, malachite.
	26.13-33.13	Shale. Color: gray. Texture: fissile, very fine-grained. Mineralogy: clay and quartz.
	33.13-40.25	Shale. Color: red-brown. Texture: very fine-grained.
MJ	0.00-7.00	Gypsum. Color: light green. Mineralogy: alabaster.

APPENDIX I (continued)

Pit	Interval (inches)	Description
MJ	7.00-26.00	Shale. Color: gray-green.
	26.00-29.00	Shale. Color: red. Texture: fissile, very fine-grained.
	29.00-31.25	Shale: Color: gray-green.
	31.25-33.75	Shale. Color: maroon. Texture: very fine-grained.
	33.75-44.25	Shale and Gypsum. From 33.75 to 35.00 inches is gray Gypsum. From 35.00 to 44.25 inches is shale. Color: gray. Texture: laminated, fissile, very fine-grained.
	44.25-61.25	Meadows Copper Shale. Color: gray with bright green spots and films on bedding and joint planes. Texture: fissile, very fine-grained. Mineralogy: clay and quartz, etc., 90%, malachite 10%.
	61.25-down	Shale. Color: gray. Texture: very fine-grained, blocky, nonlaminated.
MK	0.00-14.75	Soil, weathered Gypsum, and weathered gray Shale.
	14.75-25.50	Shale. Badly weathered. Color: light gray. Texture: fissile, very fine-grained.

APPENDIX I (continued)

Pit	Interval (inches)	Description
MK	25.50-26.50	Shale. Color: gray. Texture: sandy.
	26.50-31.00	Shale. Color: gray, base of color not strictly parallel bedding. Texture: fissile.
	31.00-38.50	Shale. Color: maroon, neither top not bottom is strictly parallel the bedding.
	38.50-42.00	Shale. Color: gray on weathered surface, maroon mottled with gray on fresh surface.
	42.00-44.00	Sandy shale. Color: red-brown. Texture: fissile.
	44.00-49.00	Shale. Color: red. Texture: very fine-grained.
	49.00-62.25	Shale. Color: gray, with yellow-orange stains on fissility planes.
	62.25-73.25	Meadows Copper Shale. Color: gray with bright green spots and films or yellow-orange films on fissility planes. Mineralogy: malachite about 10%. Includes Dolarenite layer between 69.75 and 70.00 inches.
	73.25-down	Shale. Color: gray. Texture: very fine-grained, fissile.

APPENDIX I (continued)

Pit	Interval (inches)	Description
ML	0.00-15.00	Soil, parent material was probably gray shale.
	15.00-43.00	Shale. Badly weathered. Color: gray.
	43.00-44.00	Gypsum.
	44.00-48.00	Shale. Color: red-brown.
	48.00-50.50	Gypsum.
	50.50-61.50	Shale. Color: gray.
	61.50-63.5?	Shale. Color: red-brown. Texture: very fine-grained.
MM	0.00-17.50	Soil and subsoil. Between 0.00 and 11.50 inches, parent material is gray shale. Between 11.50 and 17.50 inches, parent material is red shale.
	17.50-28.00	Shale. Color: gray. Texture: fissile, very fine-grained.
	28.00-31.50	Meadows Copper Shale (Upper Part). Color: gray, with green spots and films on bedding planes.
	31.50-32.75	Shale. Barren. Color: gray.
	32.75-34.00	Shale. Color: gray. Texture: fissile.

APPENDIX I (continued)

Pit	Interval (inches)	Description
MM	34.00-34.25	Sandstone. Color: pink. Mineralogy: quartz.
	34.25-36.50	Meadows Copper Shale (Lower Part). Color: gray with bright green spots. Texture: fissile, very fine-grained. Mineralogy: clay, quartz, and malachite.
	36.50-38.75	Sandstone. Color: yellow. Texture: one bed, medium-grained. Mineralogy: about 80% quartz.
	38.75-46.??	Shale. Color: gray. Texture: very fine-grained, fissile.
MN	0.00-11.25	Soil. Parent material is gray shale and Marty Dolomite.
	11.25-15.50	Shale. Badly weathered. Color: light gray. Very fine-grained.
	15.50-22.50	Shale. Color: mottled, more reddish at top and grayish at base. Texture: fissile, very fine-grained.
	22.50-24.50	Shale. Badly weathered. Color: gray. Texture: fissile, very fine-grained.
	24.50-28.00	Shale. Badly weathered. Color: maroon. Texture: very fine-grained, fissile.

APPENDIX I (continued)

Pit	Interval (inches)	Description
MN	28.00-43.00	Shale. Badly weathered. Color: interbedded light gray and maroonish-gray. Texture: very fine-grained, fissile.
	43.00-53.75	Shale. Color: red on fresh surface. Texture: fissile.
	53.75-66.50	Shale. Color: dark gray on fresh surface. Yellow-gray films on bedding. Texture: very fine-grained, laminated, laminae 1/8 to 1/4 inch thick.
	66.50-72.00	Meadows Copper Shale. Color: dark gray on fresh surface, with bright green spots and films on bedding surfaces. Texture: interlaminated with sand. Shale layers very fine-grained, whole rock fissile.
	72.00-72.50	Sandstone.
	72.50-75.5?	Shale. Color: dark gray. Texture: very fine-grained, fissile.
MO	0.00-10.50	Soil and subsoil. Parent material apparently gray-green shale. White films of $CaCO_3$ on joints below 6.00 inches.

APPENDIX I (continued)

Pit	Interval (inches)	Description
MO	10.50-14.00	Shale. Badly weathered. Color: dark green.
	14.00-18.50	Shale. Badly weathered. Color: maroon. Texture: very fine-grained.
	18.50-21.00	Shale. Color: dark green. Texture: very fine-grained, fissile.
	21.00-24.75	Sandy shale. Color: mottled, red-brown at top, light green at base, colors not stratigraphically confined. Texture: medium-grained, laminated, laminae about 1/8 th inch thick.
	24.75-25.25	Sandy shale. Color: red-brown. Texture: laminated, laminae usually about 1/8 th inch thick.
	25.25-27.75	Sandy shale. Color: light gray-green. Texture: laminated. Laminae about 1/8 th inch thick.
	27.75-30.50	Sandy shale. Color: red-brown.
	30.50-44.50	Shale. Color: gray with many brownish-orange stains on bedding. Texture: fissile, very fine-grained.

APPENDIX I (continued)

Pit	Interval (inches)	Description
MO	44.50-44.75	Sandstone. Color: Yellow with many bright green flakes. Mineralogy: quartz 90%, malachite 10%.
	44.75-50.50	Meadows Copper Shale. Color: gray with yellow stains, also contains bright green specks on bedding planes. Texture: very fine-grained, fissile. Mineralogy: clay and quartz 90%, limonite (?) 5%, malachite 5%.
	50.50-58.75	Shale. Color: light gray-green. Texture: very fine-grained, fissile. Includes 1/4 inch light yellow sandstone at top of interval.
	58.75-down	Shale. Color: red-brown.
MP	0.00-9.00	Material excavated from pit.
	9.00-10.00	Gypsum. Fine-grained selenite.
	10.00-18.25	Gypsiferous shale. Color: red.
	18.25-22.50	Gypsum. Color: white. Texture: fine-grained, massive, friable. Mineralogy: nearly pure alabaster.

APPENDIX I (continued)

Pit	Interval (inches)	Description
MP	22.50-30.50	Gypsiferous shale. Color: red mottled with light gray-green. Mottling irregular. Texture: very fine-grained, fissile. Mineralogy: gypsum 30%.
	30.50-40.00	Shale. Color: gray with orange-red films on fissility planes. Texture: very fine-grained, fissile, laminated, laminae about 1/8 th inch thick.
	40.00-57.50	Meadows Copper Shale. Color: gray with bright green spots on fissility planes. Texture: very fine-grained, fissile. Mineralogy: malachite 5%.
	57.50-58.00	Dolarenite layer. Color: yellow-orange.
	58.00-59.00	Shale. Color: gray.

APPENDIX II

MINERALOGICAL COMPOSITION OF THE MANGUM SAMPLES

All values in weight percent

Sample (inches)	Quartz	Gypsum	Illite	Chlorite	Malachite
MA					
0.00-12.50	26	2	58	14	0
12.50-17.00	22	2	56	20	0
17.00-20.00	28	11	53	8	0
20.00-25.00	26	13	51	10	0
25.00-32.00	24	9	26	41	0
32.00-41.25	34	19	45	2	0
41.25-52.25	25	6	59	9	1
66.25-52.25	33	1	51	13	2
66.75-69.75	21	1	56	20	2
MB					
20.00-40.25	27	15	53	5	0
41.75-64.00	28	6	55	11	0
64.00-71.00	16	17	40	27	0
MC					
19.00-33.00	23	23	26	28	0
38.50-44.25	23	5	56	16	0
46.25-49.25	27	8	54	11	0
49.25-53.25	32	0	53	15	0
53.25-56.00	24	11	51	14	0
56.00-66.00	28	11	24	37	0
68.00-68.??	18	10	37	35	0
MD					
14.50-23.75	27	39	35	0	0

APPENDIX II (continued)

Sample (inches)	Quartz	Gypsum	Illite	Chlorite	Malachite
MD					
23.75-35.25	23	5	53	19	0
35.25-44.50	29	6	48	15	2
48.25-59.50	24	5	59	11	1
ME					
21.25-26.00	26	12	53	9	0
31.13-37.25	29	27	47	0	1
37.25-40.38	22	5	27	46	0
42.75-45.25	42	32	34	0	0
45.25-52.25	25	19	45	11	0
52.25-54.75	39	5	56	0	0
54.75-55.88	35	3	55	7	0
55.88-62.25	32	7	56	5	0
62.75-65.75	35	5	55	3	2
71.50-73.50	25	9	58	8	0
MF					
33.50-36.00	25	19	38	18	0
36.00-53.13	30	8	56	6	0
53.13-61.00	26	8	56	7	3
61.00-63.00	26	8	60	6	0
MG					
24.50-42.00	14	46	32	8	0
42.00-52.00	29	6	56	8	1
52.00-61.25	26	22	46	1	5
61.25-67.00	20	21	50	8	1
52.00-55.00	29	10	52	3	6
55.00-58.00	30	29	40	0	5
58.00-61.25	15	49	29	0	7
MH					
23.75-41.25	28	32	31	9	0
47.50-61.25	32	33	33	2	0

APPENDIX II (continued)

Sample (inches)	Quartz	Gypsum	Illite	Chlorite	Malachite
MH					
61.25-78.00	30	10	53	7	0
81.25-86.00	25	28	44	2	1
86.00-89.00	23	15	53	8	1
MI					
3.50- 0.00	31	22	41	5	1
0.00- 3.88	32	2	56	9	1
6.63-12.25	25	5	52	16	2
12.25-17.25	25	3	54	16	2
17.25-21.25	27	3	54	11	5
21.25-26.13	26	7	46	14	7
26.13-33.13	25	1	59	14	1
33.13-40.25	28	10	52	10	0
MJ					
26.00-29.00	24	44	24	8	0
29.00-31.25	21	52	27	0	0
31.25-33.25	12	73	26	0	0
33.75-44.25	21	16	49	13	1
44.25-49.25	25	8	53	12	2
49.25-55.25	23	27	41	4	5
55.25-61.25	23	30	39	0	9
61.25-61.??	26	12	59	2	1
MK					
14.75-31.00	30	8	52	9	1
31.00-42.00	27	7	52	14	0
42.00-44.00	28	4	33	35	0
44.00-49.00	26	26	35	13	0
49.00-62.25	27	11	53	7	2
62.25-65.25	25	11	51	11	2
65.25-69.75	24	13	48	12	3
69.75-73.75	22	32	39	6	1
73.75-73.??	19	5	59	16	1
44.00-47.00	38	10	48	4	0

APPENDIX II (continued)

Sample (inches)	Quartz	Gypsum	Illite	Chlorite	Malachite
ML					
15.00-22.00	11	0	30	58	1
22.00-29.00	15	40	31	14	0
44.00-48.00	37	13	50	0	0
48.00-61.50	32	6	53	9	0
61.50-63.50	27	11	52	10	0
MM					
17.50-28.00	26	4	57	12	1
28.00-31.50	35	3	50	10	2
31.50-32.75	14	29	24	32	1
32.75-34.00	29	29	40	1	1
34.25-36.50	32	3	52	11	2
36.50-38.75	40	5	33	21	1
38.75-38.??	21	4	52	22	1
MN					
24.50-28.00	31	3	52	14	0
28.00-43.00	24	3	48	25	0
43.00-53.75	36	5	48	11	0
53.75-66.50	29	9	56	6	0
66.50-69.00	38	5	51	1	5
69.00-72.00	23	10	48	10	9
72.50-75.50	18	10	58	12	2
MO					
10.50-14.00	28	3	53	11	0
14.00-18.50	26	4	54	16	0
25.25-27.75	30	5	45	20	0
27.75-30.50	39	22	39	0	0
30.50-44.50	28	12	54	6	0
44.50-47.00	21	0	44	34	1
47.00-50.50	26	2	52	15	5
50.50-58.75	22	7	56	13	2

APPENDIX II (continued)

Sample (inches)	Quartz	Gypsum	Illite	Chlorite	Malachite
MP					
22.50-30.50	7	73	20	0	0
30.50-40.00	13	19	53	15	0
40.00-45.75	33	4	54	8	1
45.75-49.50	24	25	40	10	1
49.50-53.50	21	35	36	7	1
53.50-57.50	27	19	45	7	2

APPENDIX III CHEMICAL ANALYSES OF MANGUM SAMPLES

nd means "not determined."

Sample (inches)	CuO	ZnO	Ag	Pb	U	V	Co	Ni	total Fe as Fe_2O_3	K_2O	CaO	MoO_3	Organic Matter
	wt.%	wt.%	ppm	ppm	wt.%	ppm	ppm	ppm	wt.%	wt.%	wt.%	wt.%	wt.%
MA													
0.00-12.50	0.17	.038	38	32	.010	125	19	59	6.55	4.48	1.89	.013	1.85
12.50-17.00	0.19	.041	42	27	.010	176	25	58	7.18	4.38	0.80	.011	1.59
17.00-20.00	0.14	.039	39	20	.009	156	22	59	6.73	4.08	3.52	.012	0.87
20.00-25.00	0.26	.039	36	23	.010	132	16	53	5.94	3.93	4.63	.012	1.62
25.00-32.00	0.21	.032	26	16	.010	48	4	24	3.09	2.04	nd	.012	1.23
32.00-41.25	0.18	.038	39	25	.009	148	44	46	6.21	3.53	6.15	.013	0.49
41.25-52.25	0.38	.042	43	22	.010	147	19	63	6.50	4.58	1.99	.011	nd
52.25-66.25	1.58	.038	37	110	.007	132	31	60	5.51	3.95	3.56	.011	1.61
66.75-69.75	1.55	.039	39	62	.009	143	23	61	6.04	4.36	3.34	.011	1.80
MB													
20.00-40.25	0.16	.038	33	18	.009	127	14	42	5.74	4.10	5.02	.013	0.36
41.75-64.00	0.19	.040	42	40	.010	162	22	53	5.91	4.25	3.29	.014	2.02
64.00-71.00	0.15	.036	23	21	.008	90	12	28	6.14	3.14	12.42	.012	nd
MC													
19.00-33.00	0.14	.033	16	15	.010	66	0	16	3.15	2.00	nd	.012	nd
38.50-44.25	0.17	.038	37	37	.010	164	24	58	6.55	4.38	3.22	.014	0.74
46.25-49.25	0.20	.038	38	24	.010	146	23	64	6.15	4.20	3.20	.013	0.87
49.25-53.25	0.20	.020	44	18	.010	162	20	58	7.05	4.11	2.72	.012	1.46
53.25-56.00	0.23	.039	41	27	.011	142	18	64	5.91	3.93	2.38	.012	2.06
56.00-66.00	0.19	.030	15	10	.013	28	2	23	2.87	1.88	nd	.006	nd
68.00-68.??	0.14	.035	nd	25	.009	82	14	34	5.44	2.85	11.84	.011	nd

APPENDIX III (continued)

Sample (inches)	CuO	ZnO	Ag	Pb	U	V	Co	Ni	total Fe as Fe_2O_3	K_2O	CaO	MoO_3	Organic Matter
	wt.%	wt.%	ppm	ppm	wt.%	ppm	ppm	ppm	wt.%	wt.%	wt.%	wt.%	wt.%
MD													
14.50-23.75	0.18	.035	13	24	.008	97	14	26	5.49	2.69	12.55	.009	nd
23.75-3 .25	0.20	.041	38	13	.009	142	15	54	6.25	4.15	4.20	.009	1.36
35.25-44.50	1.51	.035	44	80	.007	116	28	54	5.16	3.73	5.10	.011	1.99
48.25-59.50	0.67	.042	39	27	.010	176	24	66	6.41	4.58	1.74	.009	2.05
ME													
21.25-26.00	0.29	.040	37	27	.009	109	24	51	7.51	4.11	3.76	.012	1.83
31.13-37.25	0.37	.037	29	18	.010	109	13	47	4.85	3.66	8.78	.010	1.18
37.25-40.38	0.24	.032	39	17	.009	49	1	24	2.49	2.06	nd	.011	1.04
42.75-45.25	0.16	.033	32	20	.010	106	12	38	5.02	2.61	10.58	.011	1.17
45.25-52.25	0.15	.038	19	28	.010	117	21	44	7.27	3.51	6.30	.010	0.35
52.25-54.75	0.15	.040	45	24	.010	129	24	57	6.80	4.33	1.59	.011	0.67
54.75-55.88	0.13	.040	53	26	.009	140	28	56	7.82	4.31	1.03	.012	1.74
55.88-62.25	0.25	.039	43	25	.010	127	19	59	6.30	4.35	2.38	.011	1.91
62.75-65.75	1.59	.036	43	26	.010	146	17	65	5.64	4.30	2.36	.011	2.17
71.50-73.50	0.19	.038	33	25	.009	125	24	54	7.75	4.49	2.77	.011	2.48
MF													
33.50-36.00	0.16	.034	19	19	.009	104	16	33	6.33	2.94	10.37	.007	nd
36.00-53.13	0.14	.040	45	17	.009	119	18	55	6.58	4.33	2.48	.009	1.98
53.13-61.00	2.08	.038	39	17	.009	130	14	63	5.69	4.31	2.63	.009	1.76
61.00-63.00	0.13	.038	33	20	.009	156	28	51	7.75	4.63	2.64	.009	1.91
MG													
24.50-42.00	0.16	.033	23	15	.010	60	6	17	5.05	2.45	14.85	.008	nd

APPENDIX III (continued)

Sample (inches)	CuO	ZnO	Ag	Pb	U	V	Co	Ni	total Fe as Fe_2O_3	K_2O	CaO	MoO_3	Organic Matter
	wt.%	wt.%	ppm	ppm	wt.%	ppm	ppm	ppm	wt.%	wt.%	wt.%	wt.%	wt.%
MG													
42.00-52.00	0.38	.040	39	16	.010	129	20	58	6.58	4.38	1.91	.012	2.26
52.00-61.25	3.36	.034	21	26	.009	108	6	48	4.35	3.54	7.06	.010	nd
61.25-67.00	0.70	.038	36	17	.010	110	13	47	4.76	3.85	6.85	.011	nd
52.00-55.00	4.55	.034	20	22	.009	112	16	64	5.12	4.01	3.27	.009	1.29
55.00-58.00	3.50	.030	24	22	.008	73	3	43	3.60	3.10	9.45	.010	nd
58.00-61.25	4.71	.026	1	50	.008	51	0	34	2.36	2.26	nd	.007	nd
MH													
23.75-41.25	0.26	.033	40	20	.010	65	2	29	2.92	2.39	13.20	.013	nd
47.50-61.25	0.16	.035	25	11	.009	83	9	36	5.47	2.60	10.71	.012	nd
61.25-78.00	0.28	.026	35	12	.009	110	15	55	5.77	4.08	3.74	.013	2.09
81.25-86.00	1.02	.020	25	18	.010	134	10	44	3.89	3.41	9.54	.013	nd
86.00-89.00	0.53	.038	29	17	.010	122	15	61	5.44	4.11	4.88	.013	1.52
MI													
3.50-0.00	0.35	.036	42	12	.010	101	6	41	3.84	3.20	11.72	.008	1.34
0.00-3.88	0.52	.040	56	24	.009	134	24	63	6.56	4.38	1.22	.010	2.50
6.63-12.25	1.14	.043	51	85	.007	134	23	69	6.11	4.08	2.37	.011	2.43
12.25-17.25	1.76	.041	55	84	.008	159	25	72	6.11	4.23	2.10	.009	2.76
17.25-21.25	3.46	.039	37	140	.006	127	37	67	6.45	4.20	1.04	.008	2.64
21.25-26.13	4.88	.033	26	66	.007	106	14	56	4.68	3.58	6.89	.008	2.02
26.13-33.13	0.89	.042	45	22	.010	147	21	67	6.50	4.58	1.27	.009	2.34
33.13-40.25	0.19	.041	20	25	.008	145	34	40	9.67	4.01	3.13	.008	2.03

APPENDIX III (continued)

Sample (inches)	CuO	ZnO	Ag	Pb	U	V	Co	Ni	total Fe As Fe_2O_3	K_2O	CaO	MoO_3	Organic Matter
	wt.%	wt.%	ppm	ppm	wt.%	ppm	ppm	ppm	wt.%	wt.%	wt.%	wt.%	wt.%
MJ													
26.00-29.00	0.17	.033	5	14	.010	41	3	19	3.29	1.85	nd	.007	nd
29.00-31.25	0.22	.034	11	14	.009	61	0	24	2.65	2.13	nd	.010	nd
31.25-33.25	0.18	.034	17	10	.009	49	0	16	2.78	2.05	nd	.009	nd
33.75-44.25	0.58	.040	45	55	.009	103	12	60	5.20	3.80	5.28	.010	1.54
44.25-49.25	1.74	.041	43	115	.008	147	25	67	6.05	4.13	2.64	.011	1.26
49.25-55.25	3.81	.032	14	107	.008	81	19	47	4.18	3.16	8.89	.009	nd
55.25-61.25	6.43	.024	0	49	.007	69	8	39	3.74	2.99	9.89	.009	nd
61.25-61.??	0.64	.042	52	18	.010	163	22	68	6.21	4.56	1.00	.011	2.06
MK													
14.75-31.00	0.37	.042	44	30	.010	150	18	50	5.87	4.05	2.55	.008	1.32
31.00-42.00	0.27	.039	26	21	.010	161	22	54	6.68	4.01	2.32	.009	1.37
42.00-44.00	0.18	.035	37	13	.009	79	8	29	3.90	2.56	nd	.008	1.17
44.00-49.00	0.15	.034	29	21	.009	80	13	31	5.08	2.73	11.74	.008	nd
49.00-62.25	0.49	.040	33	35	.009	138	22	55	5.92	4.10	3.53	.009	1.29
62.25-65.25	1.43	.038	24	96	.007	142	38	61	5.66	3.96	4.08	.009	1.02
65.25-69.75	1.51	.035	31	118	.007	93	41	56	5.28	3.76	5.55	.008	1.71
69.75-73.75	1.98	.031	27	226	.003	88	52	47	4.65	3.06	10.39	.007	nd
73.75-73.??	0.81	.044	32	50	.009	165	25	60	6.55	4.55	1.69	.008	1.76
44.00-47.00	0.24	.038	34	22	.010	149	19	57	5.67	3.76	3.29	.009	1.37
ML													
15.00-22.00	0.38	.034	26	78	.008	45	14	28	3.89	2.30	nd	.009	1.22

APPENDIX III (continued)

Sample (inches)	CuO	ZnO	Ag	Pb	U	V	Co	Ni	total Fe as Fe_2O_3	K_2O	CaO	MoO_3	Organic Matter
	wt.%	wt.%	ppm	ppm	wt.%	ppm	ppm	ppm	wt.%	wt.%	wt.%	wt.%	wt.%
ML													
22.00-29.00	0.20	.017	24	12	.009	61	11	19	3.11	2.41	nd	.007	nd
44.00-48.00	0.27	.036	48	25	.010	125	15	49	5.14	3.88	4.33	.009	1.55
48.00-61.50	0.26	.038	38	20	.009	113	20	53	6.37	4.09	1.98	.011	1.48
61.50-63.50	0.21	.040	28	16	.009	119	27	51	7.37	4.01	3.49	.008	1.45
MM													
17.50-28.00	0.65	.042	48	40	.009	148	27	61	6.48	4.43	1.42	.010	1.80
28.00-31.50	1.27	.038	37	179	.006	193	42	59	5.72	3.88	1.46	.009	nd
31.50-32.75	0.44	.028	23	33	.008	40	0	15	2.25	1.88	nd	.011	nd
32.75-34.00	0.65	.033	39	35	.008	103	11	42	3.74	3.13	9.31	.010	nd
34.25-36.50	1.48	.037	51	167	.006	171	41	53	6.07	4.03	1.82	.009	1.39
36.50-38.75	0.66	.032	48	64	.008	76	14	37	2.87	2.58	11.87	.009	1.36
38.75-38.7?	0.87	.044	42	32	.010	149	24	58	6.47	4.06	1.30	.010	6.64
MN													
24.50-28.00	0.17	.040	19	24	.009	125	26	43	7.61	4.00	6.18	.013	1.63
28.00-43.00	0.16	.036	24	16	.010	118	12	41	5.34	3.76	10.06	.013	1.28
43.00-53.75	0.17	.038	27	28	.009	139	30	43	8.46	3.73	3.38	.013	1.68
53.75-66.50	0.29	.037	36	16	.010	147	24	52	6.68	4.36	2.86	.014	2.25
66.50-69.00	3.45	.035	27	24	.009	159	17	55	5.19	3.97	1.64	.014	1.87
69.00-72.00	6.44	.029	0	43	.007	149	13	49	4.50	3.73	5.62	.013	1.52
72.50-75.50	1.32	.040	21	22	.010	144	20	55	5.84	4.50	3.41	.014	1.82
MO													
10.50-14.00	0.14	.038	44	16	.010	157	20	51	6.52	4.10	2.56	.014	1.59
14.00-18.50	0.13	.042	43	19	.009	148	24	52	7.75	4.20	1.34	.014	1.72

APPENDIX III (continued)

Sample (inches)	CuO	ZnO	Ag	Pb	U	V	Co	Ni	total Fe as Fe_2O_3	K_2O	CaO	MoO_3	Organic Matter
	wt.%	wt.%	ppm	ppm	wt.%	ppm	ppm	ppm	wt.%	wt.%	wt.%	wt.%	wt.%
MO													
25.25-27.75	0.13	.036	61	15	.009	127	14	46	4.89	3.53	8.28	.014	1.37
27.75-30.50	0.15	.038	27	15	.010	103	19	39	5.96	3.03	7.06	.014	1.30
30.50-44.50	0.22	.042	48	29	.009	152	20	58	5.92	4.18	3.87	.014	1.31
44.50-47.00	0.72	.035	23	116	.006	102	24	48	4.48	3.38	10.28	.014	0.10
47.00-50.50	3.74	.036	41	267	.004	146	64	63	6.50	4.03	1.88	.014	1.49
50.50-58.75	1.10	.039	47	23	.010	131	24	61	5.92	4.35	2.42	.014	1.35
MP													
22.50-30.50	0.13	.029	24	11	.009	27	0	11	2.51	1.55	nd	.007	nd
30.50-40.00	0.22	.039	39	16	.009	129	16	48	5.63	4.10	6.17	.010	0.27
40.00-45.75	0.93	.037	26	14	.008	167	21	61	6.09	4.19	1.32	.010	1.92
45.75-49.50	1.00	.033	31	58	.008	90	16	44	4.32	3.14	8.28	.012	nd
49.50-53.50	0.87	.032	23	64	.008	82	14	40	3.83	2.83	11.33	.013	nd
53.50-57.50	1.61	.034	43	243	.004	122	28	47	5.48	3.46	6.09	.012	nd

APPENDIX IV

STRATIGRAPHIC SECTIONS OF THE CRETA QUARRIES

For locations, see Figure 4

Section	Interval (inches)	Description
CN-50		Base of Marty Dolomite
	0.00-16.75	Shale. Color: gray-green. Texture: blocky.
	16.75-25.00	Gypsum. Color: contains enough red clay to provide color. Texture: one bed, whole thickness.
	25.00-27.50	Gypsum. Color: light pink. Texture: massive.
	27.50-42.25	Shale. Color: dark brownish-gray, with yellow stains on interior.
	42.25-45.75	Shale. Color: dark gray-green. Texture: laminated.
	45.75-47.00	Gypsiferous shale. Color: dark gray-green.
	47.00-48.50	Gypsum. Laminated.
	48.50-50.00	Shale. Color: dark gray-green.

APPENDIX IV (continued)

Section	Interval (inches)	Description
CN-50	50.00-56.00	Gypsum. Strung with a little gray shale. Massive.
	56.00-72.25	Prewitt Copper shale. Color: medium gray.
CN-100		Base of Marty Dolomite.
	0.00-17.50	Shale. Color: gray. From 15.50 to 17.50 inches, it is very gypsiferous.
	17.50-25.50	Gypsiferous shale. Color: red.
	25.50-27.50	Gypsum.
	27.50-43.50	Shale. Color: dark brownish-gray. Texture: blocky.
	43.50-48.75	Shale. Color: dark gray-green. Texture: fissile, laminated (?).
	48.75-54.75	Shale. Color: dark gray-green. Texture: fissile.
	54.75-72.00	Prewitt Copper Shale. Color: light gray, includes spots of dark gray shale of few mm. length. Nonlaminated mainly. Includes at least two satinspar veinlets of up to 1/4 inch thickness.

APPENDIX IV (continued)

Section	Interval (inches)	Description
CSP-1		Base of Marty Dolomite.
	0.00-16.00	Shale. Color: gray. Texture: fissile. Includes several 1/2 inch thick, sub-horizontal satinspar veinlets.
	16.00-19.00	Shale. Color: brownish-gray. Texture: fissile.
	19.00-27.00	Shaly gypsum. Color: shale partings are red. Includes a 3 inch alabaster bed at top.
	27.00-38.75	Claystone. Color: brown.
	38.75-46.00	Shale. Color: dark green. Texture: fissile, laminated. Includes gypsum bed between 44.00 and 44.50 inches.
	46.00-56.00	Gypsum and shale. Color: interbedded shale is gray. Top is 80% gypsum 20% gypsiferous shale. Base is 30% gypsum, 70% gypsiferous shale. Includes satinspar veinlets to 1 inch thickness.
	56.00-67.50	Prewitt Copper Shale. Color: dark greenish-gray.
CSP-2		Base of Marty Dolomite.

APPENDIX IV (continued)

Section	Interval (inches)	Description
CSP-2	0.00-18.75	Shale. Color: medium greenish-gray. Upper inch is mottled red, in 1 inch long blotches. Texture: fissile, laminated.
	18.75-21.75	Shale. Color: dark brown.
	21.75-27.00	Gypsum. Texture: massive.
	27.00-28.50	Claystone. Color: red. Texture: blocky, nonlaminated.
	28.50-29.50	Shaly gypsum. alabaster.
	29.50-45.50	Claystone. Color: dark brown. Texture: blocky, nonlaminated from 29.50 to 42.25 inches. Laminated below 42.25 inches.
	45.50-53.50	Shale. Color: dark green. Texture: laminated.
	53.50-62.50	Gypsum.
	62.50-74.50	Prewitt Copper Shale. Color: dark greenish-gray, with few mm. diameter gray films on joints.
	———	
CSP-3		Base of Marty Dolomite.
	0.00-1.00	Gypsum.

APPENDIX IV (continued)

Section	Interval (inches)	Description
CSP-3	1.00-17.00	Shale. Color: dark gray-green. Texture: laminated between 1.00 and 6.00 inches, blocky between 6.00 and 17.00 inches. Includes 1.50 inch satinspar veinlet between 2.00 and 2.50 inches.
	17.00-21.25	Claystone. Color: dark brown. Texture: blocky, nonlaminated.
	21.25-27.25	Gypsum. Texture: massive.
	27.25-41.50	Shale. Color: dark brown. Texture: blocky. Mineralogy: on weathered surface, forms 1 mm. beads of gypsum.
	41.50-48.00	Shale. Color: dark gray-green.
	48.00-53.25	Gypsum. Texture: massive.
	53.25-64.50	Prewitt Copper Shale. Color: dark gray-green.
CSP-4		Base of Marty Dolomite.
	0.00-1.25	Shale. Color: gray.
	1.25-3.25	Gypsum. From 1.25 to 2.50 inches, is alabaster bed. Between 2.50 and 2.75 inches, the rock is gray shale, and from 2.75 to 3.25 inches the rock is a satinspar veinlet.

APPENDIX IV (continued)

Section	Interval (inches)	Description
CSP-4	3.25-20.75	Shale. Color: gray. Texture: laminated between 3.25 and 9.25 inches, blocky below 9.25 inches.
	20.75-27.00	Gypsum. Texture: massive. Includes red shale from 23.50 to 25.00 inches.
	27.00-36.50	Claystone. Color: dark brown. Texture: massive, nonlaminated, blocky.
	36.50-44.00	Shale. Color: dark greenish-gray. Texture: blocky, laminated.
	44.00-51.25	Gypsum. From 44.00 to 47.00 inches, alabaster. From 47.00 to 48.25 inches, satinspar. From 48.25 to 50.25 inches, Prewitt Copper shale. Basal unit, from 50.25 to 51.25 inches is a satinspar layer.
	51.25-67.25	Prewitt Copper Shale. Color: gray. Mineralogy: chalcocite 5%.
	67.25-down	Shale. Color: red-brown.
CSP-5		Base of Marty Dolomite.
	0.00-22.50	Shale. Color: gray-green, includes malachite-flecked upper copper bed between 2.5 and 4.5 inches. Includes 3 subhorizontal satin-

APPENDIX IV (continued)

Section	Interval (inches)	Description
CSP-5	0.00-22.50	spar veinlets near the top. Texture: fissile.
	22.50-27.00	Shale. Color: red. Texture: very fine-grained matrix around 1/4 inch blebs of gypsum (?), fissile, nonlaminated.
	27.00-41.75	Shale. Color: dark brown, yellow-stained on small curving joint planes. Texture: fissile, nonlaminated.
	41.75-46.00	Shale. Color: dark greenish-gray. Texture: fissile, nonlaminated.
	46.00-54.50	Gypsum. alabaster.
	54.50-76.25	Prewitt Copper Shale. Color: gray. Mineralogy: chalcocite 5%. From 54.50 to 60.50 inches, rock is at least 40% gypsum in satinspar veinlets.
	76.25-down	Shale. Color: red.

APPENDIX V

MINERALOGICAL COMPOSITION OF THE CRETA SAMPLES

All values in weight percent
nd means "not determined."

Sample (inches)	Quartz	Gypsum	Illite	Chlorite	Chalcocite
CN-50					
0.00-16.75	nd	4	57	nd	0
27.50-42.25	25	1	60	14	0
42.25-45.75	25	4	57	14	0
56.00-61.00	16	27	45	6	6
61.00-67.25	26	0	62	10	2
67.25-72.25	27	3	63	7	0
CN-100					
0.00-17.50	25	1	56	18	0
17.50-25.50	24	9	46	21	0
27.50-43.50	24	3	58	15	0
43.50-48.75	22	6	56	16	0
48.75-54.75	1	87	12	0	0
54.75-60.75	13	33	41	9	4
60.75-66.00	23	5	61	11	0
66.00-72.00	25	5	61	9	0
CSP-1					
0.00-16.00	20	6	54	20	0
27.00-38.75	26	1	58	15	0
38.75-46.00	26	4	56	14	0
46.00-56.00	1	93	6	0	0
56.00-62.00	20	15	52	9	4

APPENDIX V (continued)

Sample (inches)	Quartz	Gypsum	Illite	Chlorite	Chalcocite
CSP-2					
0.00-18.75	25	7	55	13	0
18.75-21.75	26	1	56	17	0
29.50-45.50	27	2	58	13	0
45.50-53.50	21	12	54	13	0
62.50-74.50	24	2	62	6	6
CSP-3					
1.00- 5.00	25	18	51	6	0
5.00-11.00	24	1	59	16	0
11.00-17.00	21	9	54	16	0
17.00-21.25	30	5	55	10	0
27.25-32.25	29	1	59	11	0
32.25-37.25	28	3	61	8	0
37.25-41.50	32	1	58	9	0
41.50-48.00	25	6	57	12	0
53.25-59.00	18	38	40	0	4
59.00-64.50	28	2	63	3	4
CSP-4					
3.25- 9.25	26	6	56	12	0
9.25-14.75	19	12	55	14	0
14.75-20.75	24	5	57	14	0
23.50-25.00	27	5	53	15	0
27.00-36.50	26	3	58	13	0
36.50-44.00	26	6	58	10	0
48.25-50.25	21	28	48	1	2
51.25-56.75	18	29	47	0	6
56.75-61.75	24	2	66	6	2
CSP-5					
0.00- 7.50	30	17	52	1	0
7.50-15.00	21	2	59	18	0
15.00-22.50	28	3	57	12	0
22.50-27.00	23	1	43	33	0
27.00-41.75	27	1	58	14	0
41.75-46.00	27	3	59	11	0
60.50-76.25	31	4	63	0	2

APPENDIX V (continued)

Sample (inches)	Quartz	Gypsum	Illite	Chlorite	Chalcocite
CSP-5					
2.50- 4.50	25	9	55	9	2
A					
0.00- 3.00	6	0	35	57	2
3.00- 6.00	39	2	56	3	0
7.00- 9.00	24	1	48	23	4
9.00-12.00	22	0	51	27	0
12.00-15.00	31	2	53	14	0
15.00-17.40	51	0	38	11	0
B					
0.00- 1.10	2	66	30	0	2
1.10- 4.10	21	14	50	9	6
4.10- 7.10	38	1	59	2	0
7.10-10.10	40	0	58	2	0
10.10-11.42	40	0	57	3	0
C					
0.00- 1.20	1	78	21	0	0
1.20- 4.20	17	26	44	11	2
4.20- 7.20	35	1	57	7	0
7.20-10.20	25	9	54	12	0
D					
0.00- 3.00	5	66	29	0	0
3.00- 6.00	22	16	49	9	4
6.00- 9.00	28	7	55	10	0
9.00-12.00	44	0	55	1	0
12.00-15.00	29	6	56	9	0
15.00-18.00	25	3	60	2	0

APPENDIX V (continued)

Sample (inches)	Quartz	Gypsum	Illite	Chlorite	Chalcocite
E					
0.00- 1.80	5	53	31	9	2
1.80- 4.80	12	16	50	18	4
4.80- 7.80	35	1	54	10	0
7.80-10.80	34	0	56	10	0
10.80-16.80	45	0	53	2	0
F					
0.00- 3.00	13	17	40	26	4
3.00- 5.40	24	2	56	14	4
5.40- 8.40	39	0	57	4	0
8.40-11.40	31	1	58	10	0
11.40-14.40	24	0	65	11	0
G					
0.00- 3.00	34	0	57	9	0
3.00- 5.40	39	0	55	6	0
5.40- 6.00	14	22	44	16	4
6.00- 9.00	20	15	49	12	4
9.00-12.00	32	0	57	11	0
H					
0.00- 3.00	18	23	48	9	2
3.00- 6.00	28	0	58	14	0
6.00- 9.00	37	0	58	5	0
9.00-12.00	43	0	57	0	0
12.00-16.20	44	4	52	0	0
I					
0.00- 1.80	1	90	9	0	0
1.80- 2.40	8	29	28	35	0
2.40- 5.40	30	0	58	10	2
5.40- 8.40	32	0	61	7	0
8.40- 9.60	55	0	44	1	0

APPENDIX V (continued)

Sample (inches)	Quartz	Gypsum	Illite	Chlorite	Chalcocite
J					
0.00- 3.60	4	38	26	32	0
3.60- 6.60	28	2	56	13	1
6.60- 9.60	37	0	58	4	1
9.60-12.60	46	0	52	2	0
12.60-14.40	34	0	58	8	0
K					
0.00- 1.80	2	17	19	62	0
1.80- 4.80	17	15	47	20	1
4.80- 7.80	31	1	54	14	0
7.80-10.80	30	1	56	13	0
10.80-13.80	32	13	51	4	0
13.80-15.60	28	11	44	17	0
L					
0.00- 1.80	1	83	16	0	0
1.80- 4.80	14	21	40	23	2
4.80- 7.80	35	5	55	5	0
7.80- 9.60	25	0	62	13	0
M					
0.00- 2.40	11	1	32	54	2
2.40- 5.40	28	1	52	15	4
5.40- 8.40	35	4	55	6	0
8.40-11.40	28	0	56	16	0
11.40-14.40	28	2	57	13	0
14.40-19.20	59	0	41	0	0

APPENDIX VI CHEMICAL ANALYSES OF CRETA SAMPLES

nd means "not determined."

Sample (inches)	CuO	ZnO	Ag	Pb	U	V	Co	Ni	total Fe as Fe_2O_3	K_2O	CaO	MoO_3	Organic Matter
	wt.%	wt.%	ppm	ppm	wt.%	ppm	ppm	ppm	wt.%	wt.%	wt.%	wt.%	wt.%
CN-50													
0.00-16.75	0.40	.040	45	38	.010	118	26	56	6.08	4.38	1.35	.009	2.07
27.50-42.25	0.15	.042	46	20	.009	97	30	53	8.03	4.66	0.45	.009	3.51
42.25-45.75	0.17	.043	60	14	.010	101	38	56	6.44	4.43	1.32	.009	1.72
56.00-61.00	6.07	.028	10	42	.007	81	8	46	3.49	3.46	8.74	.006	nd
61.00-67.25	2.44	.037	24	31	.009	112	25	57	5.62	4.81	0.85	.007	2.07
67.25-72.25	0.24	.041	50	15	.010	118	19	59	5.88	4.90	1.58	.011	1.79
CN-100													
0.00-17.50	0.55	.040	47	48	.010	164	24	52	5.77	4.31	1.80	.009	0.67
17.50-25.50	0.15	.037	20	33	.009	131	30	35	9.37	3.56	2.84	.006	1.31
27.50-43.50	0.16	.042	46	13	.010	121	26	48	7.59	4.53	0.94	.009	2.57
43.50-48.75	0.15	.040	46	19	.010	128	24	49	6.28	4.38	1.96	.010	1.40
48.75-54.75	0.18	.027	0	4	.008	6	1	0	0.89	0.91	nd	.006	nd
54.75-60.75	4.22	.028	0	40	.007	74	6	41	3.20	3.15	10.78	.007	nd
60.75-66.00	0.55	.042	40	21	.010	135	21	54	5.54	4.73	1.76	.009	0.62
66.00-72.00	0.25	.040	45	11	.010	148	30	51	5.59	4.76	1.74	.009	0.84
CSP-1													
0.00-16.00	0.21	.042	37	15	.010	118	27	45	5.75	4.20	3.95	.009	1.42
27.00-38.75	0.15	.038	41	15	.010	160	22	47	7.53	4.48	1.31	.009	1.57
38.75-46.00	0.14	.041	61	20	.010	152	19	54	6.10	4.38	2.06	.011	1.29
46.00-56.00	0.19	.029	0	3	.009	0	0	2	0.56	0.51	nd	.004	1.06
56.00-62.00	4.55	.034	39	118	.006	106	20	52	4.70	4.06	5.47	.007	nd

APPENDIX VI (continued)

Sample (inches)	CuO	ZnO	Ag	Pb	U	V	Co	Ni	total Fe as Fe_2O_3	K_2O	CaO	MoO_3	Organic Matter
	wt.%	wt.%	ppm	ppm	wt.%	ppm	ppm	ppm	wt.%	wt.%	wt.%	wt.%	wt.%
CSP-2													
0.00-18.75	0.20	.041	45	188	.004	119	26	50	5.94	4.26	2.44	.009	1.32
18.75-21.75	0.15	.041	44	20	.010	135	26	43	8.16	4.35	0.93	.008	1.72
29.50-45.50	0.14	.041	40	20	.010	122	31	47	5.52	4.54	0.69	.009	1.61
45.50-53.50	0.17	.039	57	13	.010	126	14	47	5.27	4.17	3.78	.008	1.59
62.50-74.50	6.44	.038	35	56	.007	123	27	63	5.59	4.82	0.69	.007	2.28
CSP-3													
1.00-5.00	0.57	.039	48	168	.009	126	32	66	4.79	3.93	5.80	.009	0.43
5.00-11.00	0.46	.043	54	40	.010	150	28	55	6.01	4.60	1.74	.009	4.77
11.00-17.00	0.24	.038	37	14	.010	154	16	51	5.38	4.17	4.40	.008	2.09
17.00-21.25	0.17	.043	58	25	.010	133	19	53	6.27	4.29	2.17	.009	2.82
27.25-32.25	0.21	.041	40	17	.009	151	33	46	8.27	4.61	0.76	.011	2.47
32.25-37.25	0.11	.045	39	16	.009	160	25	48	7.85	4.71	0.64	.008	2.21
37.25-41.50	0.15	.038	45	16	.010	142	26	47	7.17	4.53	0.90	.009	1.86
41.50-48.00	0.17	.040	56	16	.010	148	42	56	6.48	4.41	2.49	.009	1.39
53.25-59.00	4.56	.029	0	48	.006	76	1	35	2.75	3.10	12.62	.006	0.58
59.00-64.50	4.46	.036	18	38	.008	129	19	67	5.75	4.87	0.83	.007	1.69
CSP-4													
3.25-9.25	0.67	.044	92	251	.008	110	57	67	5.82	4.35	1.92	.010	0.80
9.25-14.75	0.21	.043	50	9	.010	114	13	49	5.51	4.28	4.04	.009	1.42
14.75-20.75	0.14	.040	62	12	.010	157	22	56	6.18	4.43	1.73	.009	2.29
23.50-25.00	0.15	.037	25	24	.010	104	37	39	10.17	4.12	1.69	.006	0.41
27.00-36.50	0.16	.043	49	11	.010	133	23	51	7.66	4.54	0.84	.009	1.02
36.50-44.00	0.15	.041	37	74	.010	106	24	52	6.48	4.53	1.82	.011	0.20
48.25-50.25	1.59	.034	16	32	.008	115	6	45	3.74	3.70	9.08	.009	1.47
51.25-56.75	5.75	.031	6	47	.007	77	10	43	3.61	3.64	9.45	.006	1.74

APPENDIX VI (continued)

Sample	CuO	ZnO	Ag	Pb	U	V	Co	Ni	total Fe as Fe_2O_3	K_2O	CaO	MoO_3	Organic Matter
	wt.%	wt.%	ppm	ppm	wt.%	ppm	ppm	ppm	wt.%	wt.%	wt.%	wt.%	wt.%
CSP-4													
56.75-61.75	1.18	.040	33	22	.009	95	17	62	6.06	5.09	0.66	.009	2.01
CSP-5													
0.00-7.50	0.70	.043	44	60	.008	96	26	52	5.27	4.08	5.39	.009	nd
7.50-15.00	0.20	.045	49	30	.010	118	20	52	5.91	4.55	4.21	.009	1.56
15.00-22.00	0.13	.041	48	29	.010	114	26	54	6.42	4.44	1.96	.008	2.06
22.50-27.00	0.17	.037	24	27	.008	83	25	21	8.36	3.36	9.93	.008	1.25
27.00-41.75	0.13	.039	42	17	.010	112	27	43	7.24	4.49	2.11	.009	0.48
41.75-46.00	0.16	.041	51	16	.010	133	25	57	6.46	4.60	0.83	.009	2.62
60.50-76.25	1.54	.038	38	23	.009	118	26	62	5.79	4.86	1.38	.008	1.34
2.50-4.50	1.26	.043	42	114	.009	108	28	68	5.45	4.25	2.77	.009	1.12
A													
0.00-3.00	2.60	.016	13	150	.005	64	19	30	2.67	2.68	nd	.007	nd
3.00-6.00	0.69	.025	53	15	.010	152	18	53	5.47	4.32	0.56	.012	2.41
6.00-9.00	3.49	.023	23	128	.007	100	34	57	4.67	3.72	5.06	.011	0.01
9.00-12.00	0.28	.021	30	8	.010	105	13	42	5.21	3.99	6.26	.007	0.52
12.00-15.00	0.14	.021	27	15	.010	137	22	42	6.29	4.13	3.43	.008	1.71
15.00-17.40	0.13	.015	42	12	.011	73	13	37	3.19	2.97	6.87	.006	1.22
B													
0.00-1.10	2.06	.015	3	21	.007	48	0	20	1.89	2.31	nd	.006	nd
1.10-4.10	6.64	.027	0	62	.002	130	12	54	4.42	3.87	4.65	.007	nd
4.10-7.10	0.74	.028	56	22	.009	148	16	53	5.93	4.55	0.50	.009	0.67
7.10-10.10	0.15	.025	53	26	.010	143	15	50	5.78	4.49	0.38	.010	2.57
10.10-11.42	0.15	.025	58	20	.010	139	22	52	5.85	4.43	0.61	.010	1.39

APPENDIX VI (continued)

Sample (inches)	CuO	ZnO	Ag	Pb	U	V	Co	Ni	total Fe as Fe_2O_3	K_2O	CaO	MoO_3	Organic Matter
	wt.%	wt.%	ppm	ppm	wt.%	ppm	ppm	ppm	wt.%	wt.%	wt.%	wt.%	wt.%
C													
0.00-1.20	0.68	.011	4	23	.008	29	0	7	1.22	1.63	nd	.008	nd
1.20-4.20	2.62	.022	20	23	.008	80	7	42	3.66	3.43	8.47	.008	nd
4.20-7.20	0.23	.022	53	13	.010	131	16	55	5.74	4.43	1.48	.011	0.69
7.20-10.20	0.21	.022	46	17	.009	91	17	46	5.66	4.22	3.97	.010	0.68
D													
0.00-3.00	0.70	.014	5	14	.009	23	0	21	1.94	2.27	nd	.008	nd
3.00-6.00	4.49	.024	0	55	.008	114	11	50	4.22	3.78	5.08	.009	nd
6.00-9.00	0.53	.025	43	24	.010	102	14	47	5.35	4.25	2.35	.011	0.93
9.00-12.00	0.18	.026	51	16	.010	142	22	57	5.67	4.26	0.56	.011	1.81
12.00-15.00	0.13	.025	36	17	.011	126	20	49	5.70	4.38	1.95	.008	1.43
15.00-18.00	0.15	.023	48	24	.010	100	21	52	6.65	4.66	1.11	.010	1.80
E													
0.00-1.80	1.41	.015	25	12	.009	52	0	20	2.00	2.41	nd	.008	nd
1.80-4.80	2.95	.026	33	40	.009	79	10	46	4.30	3.88	5.45	.010	nd
4.80-7.80	0.23	.027	51	10	.010	160	18	47	5.16	4.23	1.61	.011	2.06
7.80-10.80	0.17	.026	64	21	.010	130	23	54	5.40	4.33	0.46	.012	1.83
10.80-16.80	0.13	.022	58	20	.011	125	16	48	5.29	4.10	0.54	.010	1.73
F													
0.00-3.00	3.25	.019	20	204	.004	57	19	38	3.42	3.12	11.79	.010	nd
3.00-5.40	4.34	.028	47	109	.006	123	24	60	5.27	4.32	1.95	.010	0.27
5.40-8.40	0.45	.027	57	18	.010	132	22	57	5.53	4.41	0.44	.011	1.76

APPENDIX VI (continued)

Sample (inches)	CuO	ZnO	Ag	Pb	U	V	Co	Ni	total Fe as Fe_2O_3	K_2O	CaO	MoO_3	Organic Matter
	wt.%	wt.%	ppm	ppm	wt.%	ppm	ppm	ppm	wt.%	wt.%	wt.%	wt.%	wt.%
F													
8.40-11.40	0.46	.023	55	29	.010	182	22	54	5.78	4.48	0.75	.011	1.84
11.40-14.40	0.21	.024	46	18	.010	138	26	54	7.18	5.01	0.33	.011	2.19
G													
0.00-3.00	0.22	.026	56	23	.010	138	19	55	5.59	4.43	0.47	.010	2.03
3.00-5.40	0.24	.021	57	24	.010	138	17	51	5.21	4.26	0.56	.010	1.13
5.40-6.00	3.31	.021	39	182	.004	79	29	48	4.25	3.38	7.23	.009	nd
6.00-9.00	3.75	.023	50	134	.006	120	27	53	4.84	3.81	4.97	.010	nd
9.00-12.00	0.49	.026	49	25	.010	133	19	50	5.47	4.41	0.60	.011	1.73
H													
0.00-3.00	2.29	.024	27	39	.008	77	12	42	4.18	3.70	7.43	.009	nd
3.00-6.00	0.50	.028	51	26	.010	125	24	49	6.26	4.52	0.88	.011	1.62
6.00-9.00	0.28	.027	60	17	.010	132	21	51	5.70	4.48	0.38	.012	2.15
9.00-12.00	0.17	.022	59	18	.010	141	23	53	5.56	4.45	0.40	.013	2.11
12.00-16.20	0.16	.019	51	15	.010	119	14	48	4.91	4.03	2.78	.011	1.12
I													
0.00-1.80	0.44	.008	4	62	.006	0	0	1	0.59	0.67	nd	.009	nd
1.80-2.40	0.91	.016	19	116	.006	36	11	16	2.05	2.15	nd	.010	nd
2.40-5.40	2.62	.024	41	89	.008	162	28	55	5.94	4.50	1.23	.011	1.34
5.40-8.40	0.20	.025	48	24	.010	136	24	52	7.08	4.73	0.69	.011	1.92
8.40-9.60	0.15	.016	54	25	.012	114	18	46	3.92	3.42	2.38	.010	1.07

APPENDIX VI (continued)

Sample (inches)	CuO	ZnO	Ag	Pb	U	V	Co	Ni	total Fe as Fe_2O_3	K_2O	CaO	MoO_3	Organic Matter
	wt.%	wt.%	ppm	ppm	wt.%	ppm	ppm	ppm	wt.%	wt.%	wt.%	wt.%	wt.%
J													
0.00-3.60	1.08	.016	19	141	.004	33	0	15	1.54	1.98	nd	.008	nd
3.60-6.60	2.79	.026	54	201	.006	116	47	61	6.03	4.36	2.17	.012	nd
6.60-9.60	1.90	.042	46	40	.009	144	13	57	5.52	4.53	0.71	.011	2.07
9.60-12.60	0.19	.020	67	26	.011	124	11	47	4.80	4.07	2.38	.013	1.05
12.60-14.40	0.24	.021	56	16	.010	136	12	52	5.63	4.48	1.81	.012	0.82
K													
0.00-1.80	1.44	.032	14	175	.004	2	9	19	1.59	1.52	nd	.008	nd
1.80-4.80	1.89	.022	59	391	.002	119	66	60	5.20	3.62	6.40	.010	nd
4.80-7.80	1.07	.027	64	65	.009	158	17	52	5.44	4.19	1.29	.011	nd
7.80-10.80	0.19	.022	80	24	.009	158	11	48	5.62	4.35	1.26	.012	2.04
10.80-13.80	0.21	.020	50	19	.009	101	10	45	5.20	3.95	4.27	.011	0.99
13.80-15.60	0.18	.020	52	17	.009	66	9	35	4.24	3.38	7.10	.011	nd
L													
0.00-1.80	0.69	.028	0	109	.006	3	1	15	1.18	1.27	nd	.009	nd
1.80-4.80	1.36	.024	40	177	.006	80	25	38	4.22	3.09	11.45	.010	nd
4.80-7.80	0.69	.025	63	44	.010	161	13	51	5.22	4.28	2.63	.011	0.60
7.80-9.60	0.19	.025	56	31	.010	161	17	57	6.63	4.83	0.73	.010	1.60
M													
0.00-2.40	2.08	.021	11	190	.005	13	23	29	2.41	2.46	nd	.009	0.03
2.40-5.40	3.22	.025	33	172	.006	125	38	64	5.41	4.06	2.25	.012	nd
5.40-8.40	0.50	.025	57	28	.010	120	12	53	5.16	4.26	1.36	.010	0.97
8.40-11.40	0.28	.026	59	18	.010	154	15	49	5.91	4.36	1.49	.011	0.96
11.40-14.40	0.33	.024	33	18	.009	128	19	49	6.24	4.40	1.17	.011	1.03
14.40-19.20	0.15	.014	42	17	.011	112	7	36	3.92	3.15	4.19	.009	1.27